Phase development of hydrated cement pastes with SCMs under delayed heating conditions below 100 °C

Oumayma Ahmadah, Mickael Saillio, Julien Vincent, Abdellatif Ammar, Loic Divet, Jean-Michel Torrenti, Arezki Tagnit-Hamou, Georges Nahas

Phase development of hydrated cement pastes with SCMs under delayed heating conditions below 100 °C

Oumayma Ahmadah[a], Mickael Saillio[a*], Julien Vincent[a], Abdellatif Ammar[a], Loic Divet[a], Jean-Michel Torrenti[a], Arezki Tagnit Hamou[b], Georges Nahas[c]

[a] *Université Gustave Eiffel, Departement MAST, CPDM, Champs-sur-Marne, France*
[b]*Université de Sherbrooke, Department of Civil and Building Engineering, Sherbrooke, Québec, Canada*
[c]*IRSN, Fontenay aux Roses, France*

Abstract
This paper focuses on studying the effect of the delayed heating of cementitious materials on the phase assemblage variations in three types of cement paste. Two heating temperatures of the order of 65 °C and 80 °C were used to thermal treat the samples. Our results show that the thermal treatment induces the modification of the phase assemblage (particularly degradation of AFt and AFm phases) as well as the polymerization of the C-(A)-S-H. The observed variations depend mainly on the initial sulfate, aluminate and carbonate content in each cement. Finally, it is shown that the thermal treatment-related phenomena such as adsorption of aluminates on C-(A)-S-H are almost completely reversible after the temperature drop and re-immersion in water for 3 months, meanwhile other phenomena such as the formation of the hydrogarnet and hydrotalcite are only partially reversible. This modifies the free elements proportion and influences the probability of the DEF occurrence.

**Corresponding author. Tel.: +33 1 81 66 82 39*
E-mail address: mickael.saillio@univ-eiffel.fr

1 Introduction

The early heat rise of the temperature of cementitious materials can occur either in heat treated concrete or concrete cast in place in massive parts such as for dams and bridges [1–3]. This rise in temperature at early age affects the creep as well as the thermoelastic properties of concrete. In this case, previous studies showed that these properties decrease and could affect the service life of concrete structures [4–6]. In details, as main deterioration mechanism, the temperature rise may induce a delayed ettringite formation (DEF) when the temperature exceeds 65 °C to 70 °C [1,7–12]. The DEF has often been linked to the decomposition of primary ettringite at high temperatures and then the stabilization of an expansive ettringite when the temperature drops and the structure remains in contact with a moist environment for a long time [13–16]. Many publications discussed the effect of an early temperature elevation during the hydration kinetics, the hydrate phase assemblage, microstructure and durability of the material [17–29]. In short, there was an increase of hydration process, less primary ettringite was formed and porosity could also increase. Consequently, most of publication showed that the concrete durability decreased in case of a temperature rise at young age. Nevertheless, their conclusions concerning the phase assemblage were only conducted on a limited number of phases (portlandite or C(-A)-S-H or sometimes on AFm/AFt phases). There was therefore often a lack of a global point of view which was obtained only by numerical modeling [30].
Moreover, during their service life, structures, such as facilities for nuclear waste storage, may undergo late temperature elevations that may reach the temperature of 80 °C for several years [30]. As the result, this case is quite different from the one interfering during hydration kinetics since

phase assemblage is different according age of material [29]. The mechanism is expected quite different for these two cases. However, this late temperature elevation can also affect the material phase assemblage, microstructural and transfer properties as demonstrated by authors [30-36]. Indeed, the DEF may occur in these structures, which could damage their concrete, and thus the security requirements expected could be under threat after many years of exposure [31]. In this case of delayed heating of the structure, studies investigated in particular the influence of exposure to temperatures ranging from 100 °C to 1000 °C as it is the case for fire [32–36] which is not the case of an ordinary and expected service life (which T < 100 °C). To our knowledge, only few researches studied the effect of a late temperature elevation from 65 °C to 90 °C [11,37–40]. Nonetheless, these publications only discussed the C-(A)-S-H phase modification (as water loss) or the observed swellings (causing cracks) in the material and not the evolution of the complete phase assemblage. Furthermore, researches focused mainly on applying heat treatment with a high humidity in order to reach the DEF (superior to 90%). Nevertheless, the relative humidity in concrete structures can achieve lower values in real service life. Indeed, values between 45% and 65% were estimated for the relative humidity in the surface of concrete for nuclear waste storage facilities [41].

The main objective of this study was to evaluate the effect of a delayed thermal treatment (TT) below 100 °C applied on hydrated cement pastes, regarding the phase assemblage modifications. Two temperatures, 65 °C and 80 °C, were applied on the samples for various durations from 1 day to 56 days and compared to samples left in a 20 °C climatic chamber. The relative humidity was kept at 55% in order to reproduce the same conditions for nuclear waste storage facilities. The phase assemblage was evaluated just after the thermal treatment. In addition, some characterizations were performed after re-immersion of the thermal treated samples in water for 3 months. The results were obtained using XRD, TGA-DTA, and ^{29}Si and ^{27}Al NMR spectroscopies.

2 Experimental

2.1 Materials studied

Different cement pastes were formulated with CEM I, CEM II/A-LL (with limestone) and CEM V/A (with slag and fly ash). The first two cements are usually used for the manufacture of the containment vessels of some nuclear reactors while the third one is suggested to be used in the Cigeo project for the very long-term storage of radioactive waste [41]. The main constituents of the three cements are given in Table 1, Table 2 and Table 3.
Cylindrical specimens (Ø=2 cm; H=5 cm), intended for analytical tests (XRD/TGA/NMR), were prepared using these three types of cement. All mixture were hydrated with the same water to binder ratio (w/b) equal to 0.44. This choice of the W/C ratio was inspired by industrial constraints to simulate cases of relatively low porosity cementitious materials. The cement pastes were denoted P1 (CEM I), P2 (CEM II/A) and P5 (CEM V/A). The materials were unmolded after 24 hours. The specimens were stored in water tanks, separately according to the type of used cement for at least 400 days, till the late heat treatment was applied. The cement pastes were considered fully hydrated as demonstrated by literature [29]. A long water curing was used in order to avoid a possible coupling between the hydration effect and the thermal effect which was the studied effect here (close to the real case).

Table 1. Chemical composition of the cements (in % weight) obtained by X-Ray Fluorescence spectrometry (XRF). L.O.I. loss of ignition ; I.R. insoluble residue.

	CEM I 52.5N	CEM II/A-LL 42.5R	CEM V/A (S-V) 42.5N
CaO	63.20	63.50	46.20
SiO_2	19.30	19.70	31.10

Al_2O_3	5.30	4.60	10.20
Fe_2O_3	2.60	3.20	3.60
SO_3	3.50	2.70	2.80
MgO	2.00	1.20	2.70
Na_2O	0.08	0.11	0.37
K_2O	0.94	1.36	1.27
Cl^-	0.01	0.05	0.01
S^{2-}	0.02	0.02	0.17
P_2O_5	0.20	0.50	0.40
TiO_2	0.30	0.30	0.60
L.O.I.	2.90	3.60	1.50
I.R.	0.50	< 0.01	< 0.01
$Na_2Oéq$	0.70	1.01	1.21

Table 2. Mineralogical composition of the cement clinker from BOGUE calculation (in % weight). CEM II/A and CEM V/A were made from the same manufactory (same clinker composition).

Clinker composition	CEM I 52.5N	CEM II/A-LL 42.5R	CEM V/A (S-V) 42.5N
C_3S	66	66	66
C_2S	10	11	11
C_3A	11	7	7
C_4AF	8	10	11

Table 3. Mineralogical composition of the cements (in % weight). Data are from the manufacturer.

	CEM I 52.5N	CEM II/A-LL 42.5R	CEM V/A (S-V) 42.5N
Clinker	91.0	89.5	54.3
Limestone	3.8	5.8	-
Slag (GGBS)	-	1.9	21.3
Fly ash (FA)	-	-	21.3
Gypsum	5.2	2.7	3.1

2.2 Heat treatment and Re-immersion process

A part of hydrated cement pastes was subjected to heat treatments at 65 ˚C and 80 ˚C for periods of 1 day, 3 days, 7 days, 14 days, and 28 days or 56 days. The relative humidity was kept at 55% for all samples. The thermal treatment was denoted TT. In addition, another part of cement pastes was subjected to heat treatment at 20 °C and 55% RH (as reference samples) after water curing time.

The various heat treatments were performed in climatic chambers (controlled conditions). The samples were prepared and stored under water for at least 14 months. The thermal treatments were carried out after 720 days of storage in water for the two temperatures at 20 °C and 80 °C, and after 410 days of storage in water for 65 °C. The 28 days curing time at 80 °C could not be obtained (due to COVID confinement situation) and was replaced by 56 days at 80 °C. The mass variations of samples were tracked by weighing samples before and after the TT (on single sample from each series), and the rest of characterization tests (NMR, XRD, TGA) were carried out as soon as the samples were

taken out of the climatic chamber. The experimental program is resumed in Figure 1. Thermal treated samples at 80 °C for 56 days were then re-immersed in water for 3 months at ambient temperature in order to observe the DEF occurrence and to characterize the phase assemblage afterwards.

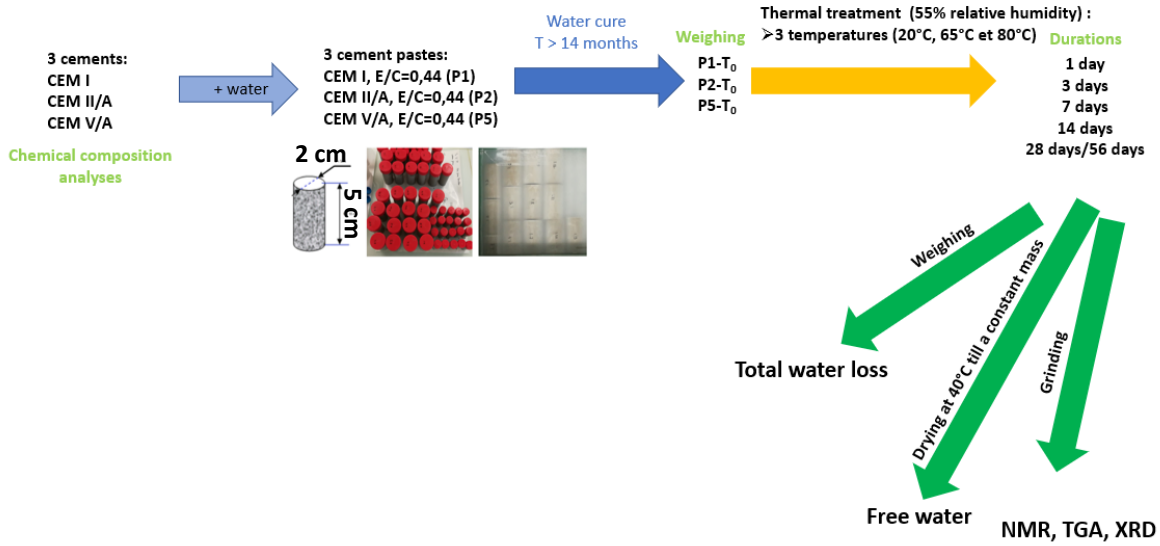

Figure 1. Graphical scheme of the experimental program.

2.3 Microstructure characterization

2.3.1 TGA- DTA

Thermogravimetric analyses (TGA) and differential thermal analyses (DTA) [29,42,43] were performed with a simultaneous thermal analyzer by heating from 25 °C to 1250 °C with 10 °C/min steps. These techniques were used to quantify the water content lost from portlandite and from C-S-H and ettringite (noted C-S-H + E), as well as the CO_2 content lost by the calcium carbonates in the samples formed during carbonation. The initial amount of cement was also obtained by measuring the remaining mass after the last CO_2 loss. The analyses were applied to crushed samples. The device used here is a NETZSCH STA 409 coupled with mass spectrometer in order to analyze the outlet gases.

2.3.2 XRD

X-ray diffraction [29,43] allows to identify the crystallized phases that are the hydrated phases from clinker hydration (e.g. portlandite, monocarboaluminate …) as well as the phases formed during thermal treatment (e.g. hydrogarnet, …) and to estimate their proportions. Such analyses were carried out here on crushed pastes. The XRD analyses were performed using Empyrean diffractometer with the Kα radiation of cobalt (40 kV and 30 mA). The scan step size of the diffractometer was 0.013 °/s in the range of 2Θ from 4 and 76°.

2.3.3 NMR

NMR spectroscopy [45] gives access, at a local scale, to the immediate environment of a nucleus. ^{27}Al and ^{29}Si nuclei were observed by the MAS (Magical Angle Spinning) technique [29,45,46]. Geometrical configurations of a nucleus are a function of the chemical shift. NMR spectra were obtained with a Bruker Avance 500 MHz apparatus (11.74 T magnetic field).

The coordination of aluminum atoms can be observed by ^{27}Al NMR [45]. In a cement paste, aluminum in tetrahedral configuration Al(IV) is generally attributed to aluminum substituted for silicon in C-S-H chains and residual anhydrous cement. Aluminum in octahedral Al(VI) configuration is divided into three components: AFt (Ettringite), AFm and the third aluminum hydrate (TAH) which is, an amorphous/disordered aluminum hydroxide or a calcium aluminate hydrate not observable by XRD. The representative resonance of aluminum in AFm phases can hardly distinguish their different forms such as Friedel's salt, monosulfoaluminate, monocarboaluminate phases and Küzel's salt. However, XRD can complement the information provided by NMR and help to identify what the involved AFm phases are. Finally, the attribution of aluminum in pentahedral configuration Al(V) is still debated but usually assigned to aluminum substituted for calcium in the C-S-H interlayers or present in non-hydrated phases.
^{29}Si MAS NMR spectra allow identification of the different connectivities of silicon tetrahedron in the samples [45]. In NMR spectroscopy, silicon tetrahedra are designated as Q^n, where Q represents the silicon tetrahedron bonded to four oxygen atoms and n denotes its connectivity, i.e. the number of other Q units attached to the SiO_4 tetrahedron under study. In cement pastes, Q^o coordination occurs in anhydrous silicates (C_3S, C_2S and also GGBS), while Q^1 and Q^2 are present in the C-S-H chains. Q^3 and Q^4 correspond to cross-linking of the dreierketten chains of C-S-H or to silicon in silica gels as observed in carbonated samples and there is also Q^4 from anhydrous FA. In the presence of Al, others species can be observed such as Q^n(mAl), where m represents the connectivity of silicon tetrahedron attached to m aluminate tetrahedra. From quantitative ^{29}Si NMR spectra, the average length of C-S-H chains can be estimated from the relative intensities of the resonances as $2 + 2 \times Q^2/Q^1$, as well as the advancement of the silicate hydration as $1\text{-}Q^0$. This last formula is quite easy to apply for hydrated CEM I where the Q^o resonance is well defined but it is more complex for a cement paste with SCMs. So, the formula is adapted considering Q^o as the sum of Q^o from clinker (C_2S and C_3S) and also the anhydrous phase of SCM (GGBS and FA). In these formulas, Q^n represents the relative integrated intensities of the resonance assigned to that particular environment. The integrated intensities were obtained by fitting the spectra using the DMFIT freeware.

2.3.4 The combined method

The method used to quantify each phase from a combination of MAS NMR spectroscopy, elementary analysis by ICP-AES and TGA/DTA is fully described in [29] and will not be reproduced here. It will be denoted as “combined method” in legend of the figures. For example, the molar stoichiometry of C-S-H (or C-A,S-H) is unknown in hydrated cement paste. Consequently, in order to calculate adequately the amount of C-S-H (or C-A,S-H), each constitutive oxide of this compound (%SiO_2, %CaO, %Al_2O_3 and %H_2O) is distinctly quantified using various analytical and spectroscopic methods for 100 g of hydrated cement paste. %SiO_2 is obtained by ^{29}Si NMR, %Al_2O_3 by ^{27}Al NMR, %H_2O by TGA. %CaO is indirectly obtained considering the total amount of calcium minus the sum of all other phases containing calcium. Concerning measurement uncertainties, they will be discussed in the results section as well as the limits of the calculation methods used here.
In the particular case of the present study, these calculations notably take into account the concentration effect provided by the water loss during the thermal treatment (determined by TGA) in order to quantify adequately the elemental composition expressed in weight oxide (%SiO_2, %CaO, …) or weight phase (portlandite, …) in the TT cement pastes.

The aim of this experimental campaign was not only to investigate the overall phase assemblage after TT and, in particular, the chemical transformations but also to have a detailed view on each phase.

3 Results and discussion

3.1 General effect of the heating treatment on the water content

Figure 2 shows the total water loss during the thermal treatment for samples P1 and P5. It was considered that the total water loss corresponds to the total mass loss during TT. As expected, the longer the sample was left in the climatic chamber, the dryer it became.
The mass losses followed similar trends for P1 (see Figure 2A and 2B) and P2 (see Figure A.1) while for P5 the mass losses was lower (see Figure 2C and 2D). For P5, these mass losses did not seem to stabilize after 28 days at 65 °C or 80 °C unlike P1 and P2. These differences were expected since the porous network before treatment was thinner and more tortuous for P5 than it was for P1 or P2 [47]. As the consequence, P5 had more difficulties losing its water during the drying than P1 or P2 (the geometries of the samples being comparable). Moreover, the initial water content of the samples was different.
When the total water loss was compared to free water loss (obtained by drying the samples at 40 °C till a constant mass), the total water lost during TT did not correspond only to a drying of the free water in samples. So, water-rich phases (such as Ettringite or C-(A)-S-H) lost a part of their water content.
In conclusion, the temperature rise obviously affected the free water content in the pores, but it also influenced the hydrated phases (a possible decrease). It probably induced an evolution of the phase assemblage. Therefore, it was also interesting to focus on equilibrium of all phases in cementitious matrix.

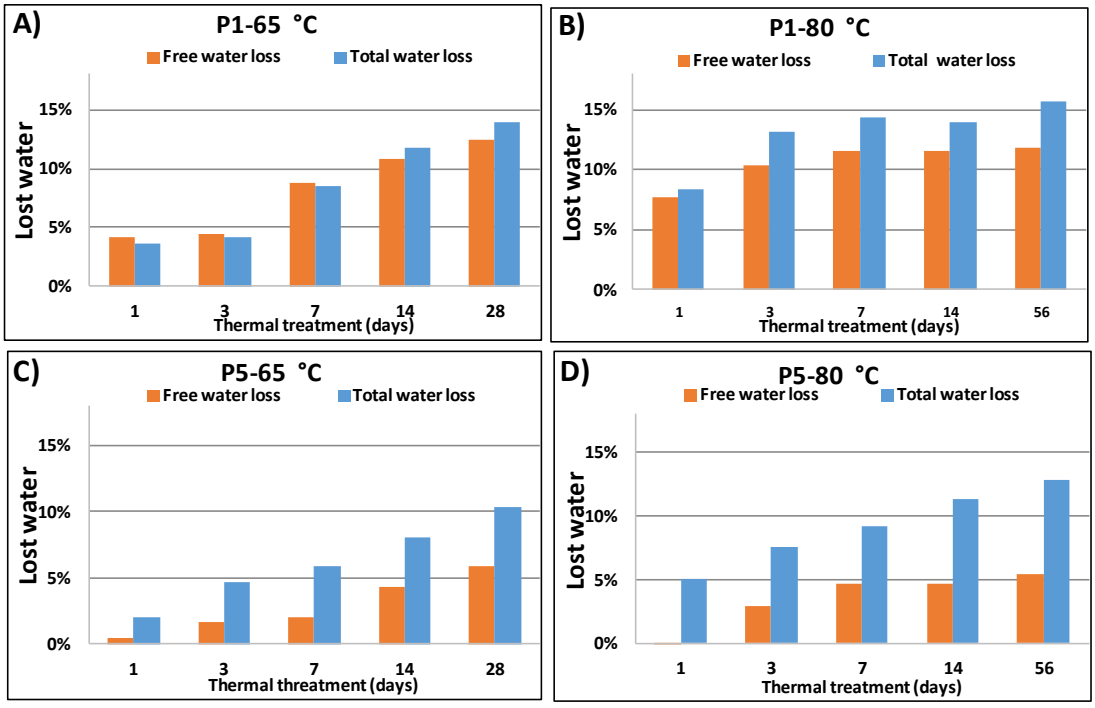

Figure 2. Free water loss and total water loss induced by the TT for samples P1 and P5.

3.2 Effect of the heating treatment on phase development

3.2.1 Comparison of the used techniques for phase assemblage characterization

The phase assemblage was obtained by the combined method (see Section 2.3.4) and by the Rietveld-analyzed XRD results [48]. The XRD technique enabled to access to the contents of the crystallized phases meanwhile the combined method allowed to quantify portlandite (using TGA method and focusing on its lost water) as well as phases containing aluminates (using ^{27}Al NMR) or silica (using ^{29}Si NMR). The combination of the results of these two techniques was a better way to

understand the phase assemblage modifications during TT. In fact, amorphous phases cannot be identified by XRD and in particular for C-(A)-S-H and this is more accurate with ^{29}Si NMR. For portlandite amount, TGA/DTA remains the best technic to be used. In addition, details of AFm phases (monocarboaluminate, monosulfoaluminate, …) are only observed by XRD and not by NMR ^{27}Al which sums all these phases in terms of AFm phases.

The proportions of each cementitious phase achieved by these two methods for various cement pastes (P1 and P5) and for different TT conditions were obtained by these methods (see Figure 3, Figure 4 and see all results for P2 in appendix A which are not presented here since they are similar to those collected on P1). Samples after the TT did not have the same mass, either by effect of drying which induced a mass concentration or by effect of partial carbonation which induced a mass dilution. Thus, the mass proportions of hydrates were reported to a reference quantity (see Figure 3 and Figure 4), which was the mass of the initial anhydrous content. The global results are useful for future modeling but given the evolution of some phases, it was difficult to directly understand the underlying mechanisms linked to TT. As the result, it was necessary to look in detail, starting with the equilibrium of aluminate phases.

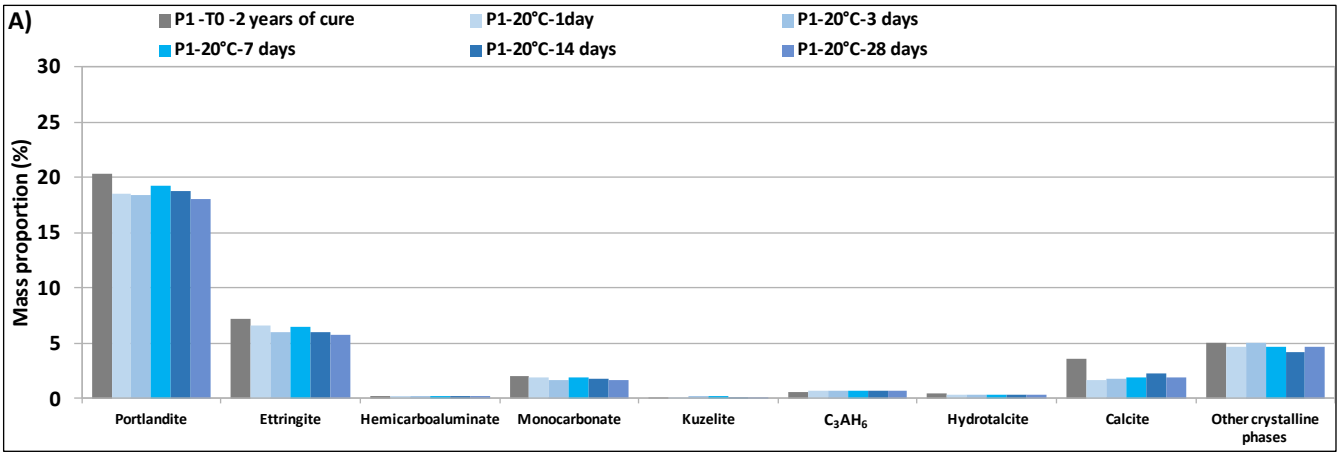
A)
P1 -T0 -2 years of cure
P1-20°C-1day
P1-20°C-3 days
P1-20°C-7 days
P1-20°C-14 days
P1-20°C-28 days
Mass proportion (%)
30
25
20
15
10
5
0
Portlandite
Ettringite
Hemicarboaluminate
Monocarbonate
Kuzelite
C_3AH_6
Hydrotalcite
Calcite
Other crystalline phases

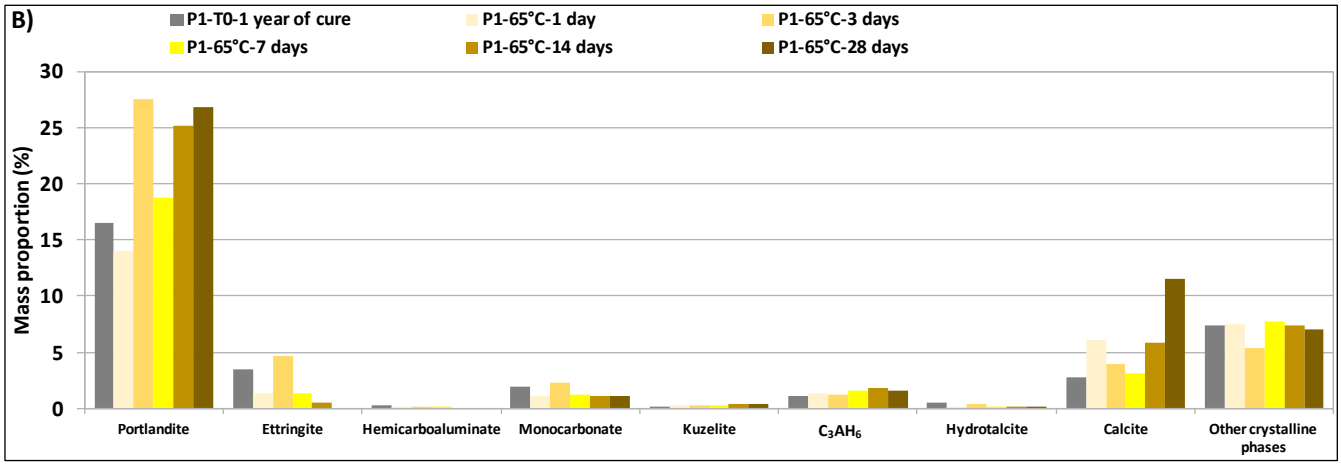
B)
P1-T0-1 year of cure
P1-65°C-1 day
P1-65°C-3 days
P1-65°C-7 days
P1-65°C-14 days
P1-65°C-28 days
Mass proportion (%)
30
25
20
15
10
5
0
Portlandite
Ettringite
Hemicarboaluminate
Monocarbonate
Kuzelite
C_3AH_6
Hydrotalcite
Calcite
Other crystalline phases

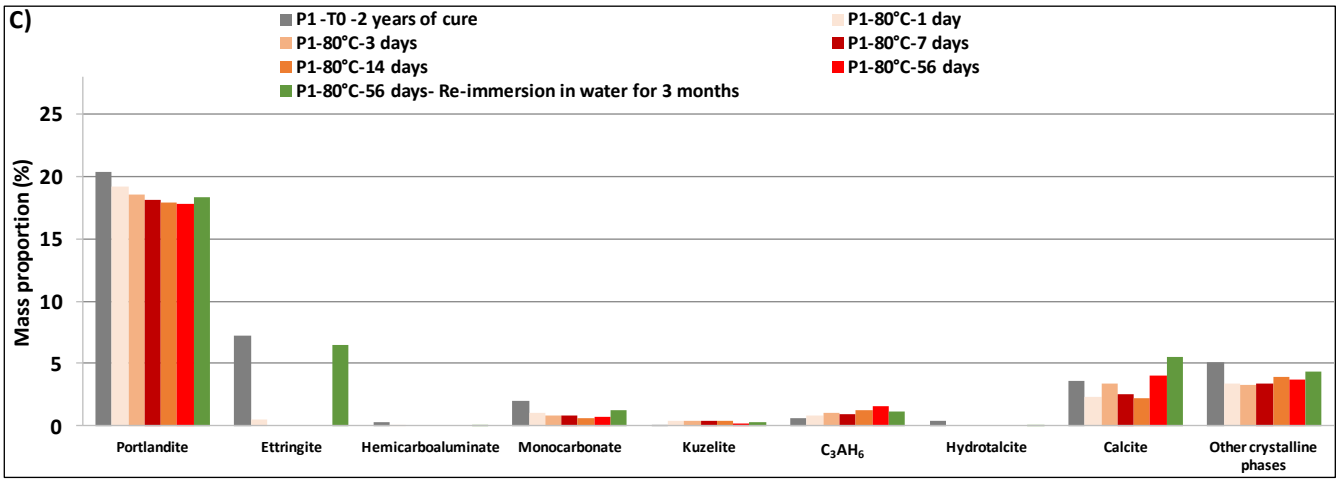
C)
P1 -T0 -2 years of cure
P1-80°C-1 day
P1-80°C-3 days
P1-80°C-7 days
P1-80°C-14 days
P1-80°C-56 days
P1-80°C-56 days- Re-immersion in water for 3 months
Mass proportion (%)
25
20
15
10
5
0
Portlandite
Ettringite
Hemicarboaluminate
Monocarbonate
Kuzelite
C_3AH_6
Hydrotalcite
Calcite
Other crystalline phases

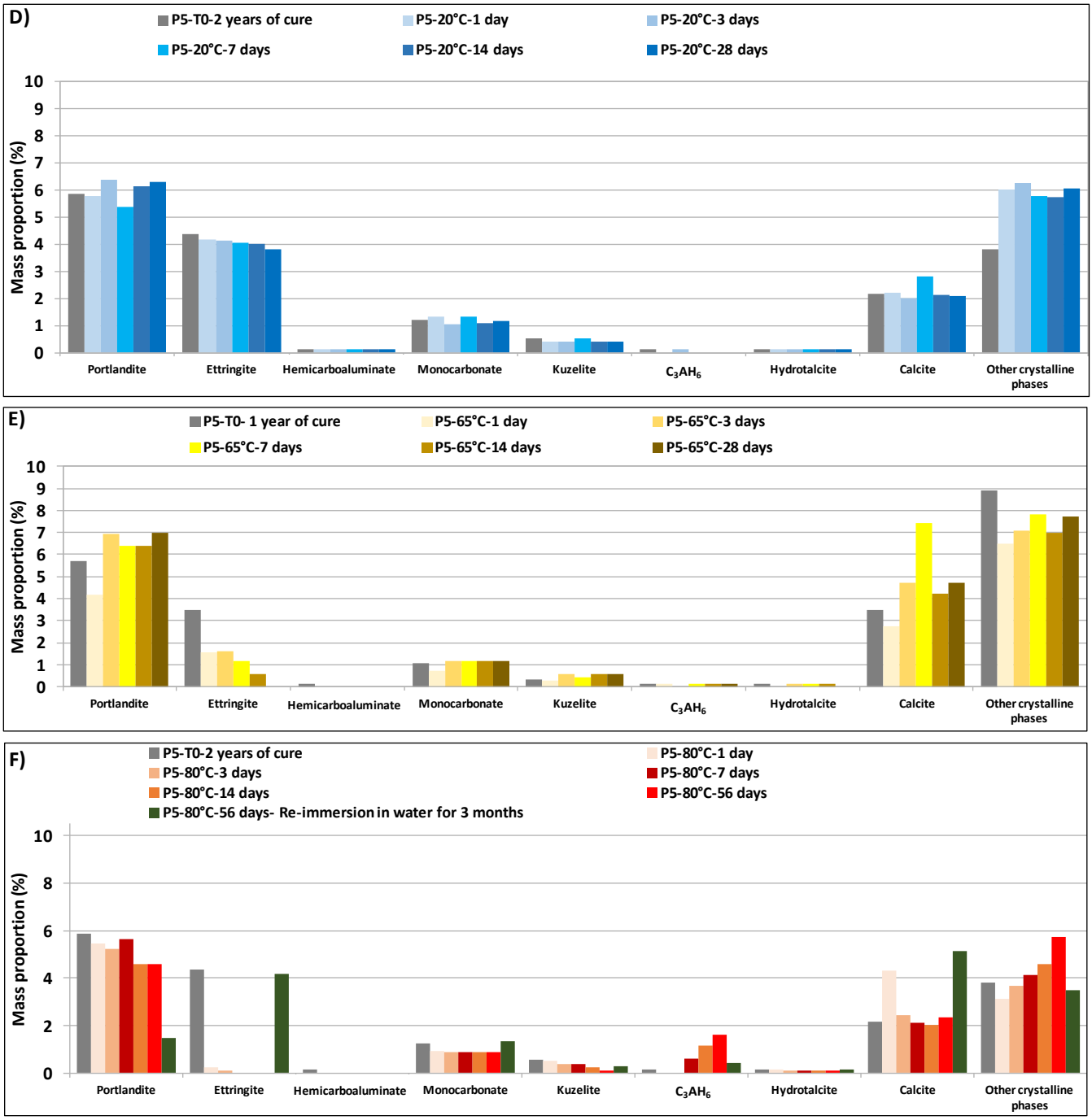

Figure 3. Evolution of the phase assemblage as a function of the TT obtained by quantitative XRD for samples P1 and P5. The mass proportion of the phase is reported to the quantity of the initial anhydrous content. Other crystalline phases: C_3S, C_2S, C_3A, C_4AF.

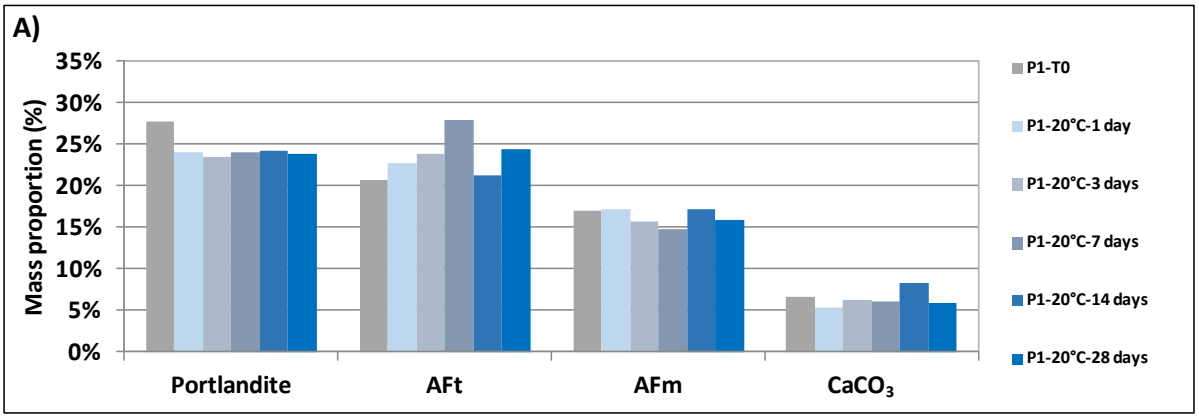
A)
Mass proportion (%)
35%
30%
25%
20%
15%
10%
5%
0%
Portlandite
AFt
AFm
CaCO3
P1-T0
P1-20°C-1 day
P1-20°C-3 days
P1-20°C-7 days
P1-20°C-14 days
P1-20°C-28 days

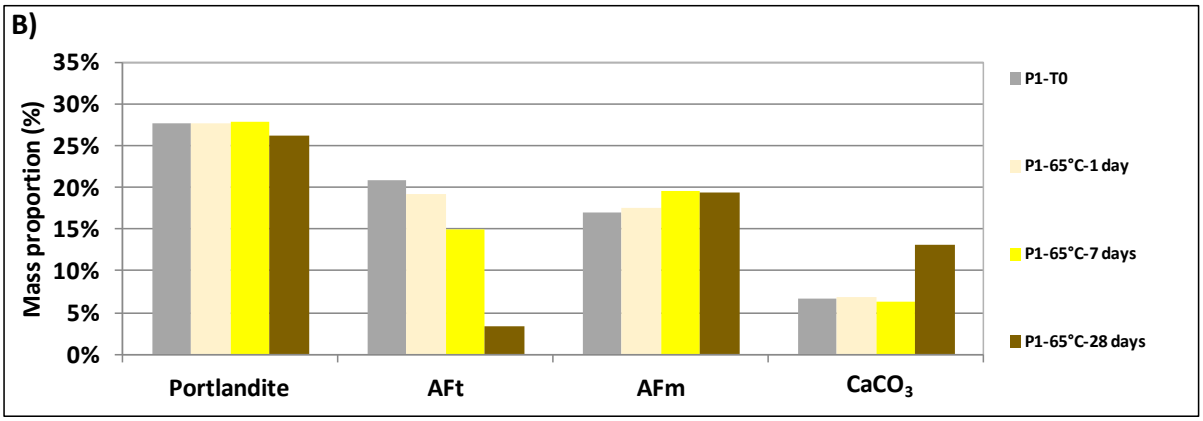
B)
Mass proportion (%)
35%
30%
25%
20%
15%
10%
5%
0%
Portlandite
AFt
AFm
CaCO3
P1-T0
P1-65°C-1 day
P1-65°C-7 days
P1-65°C-28 days

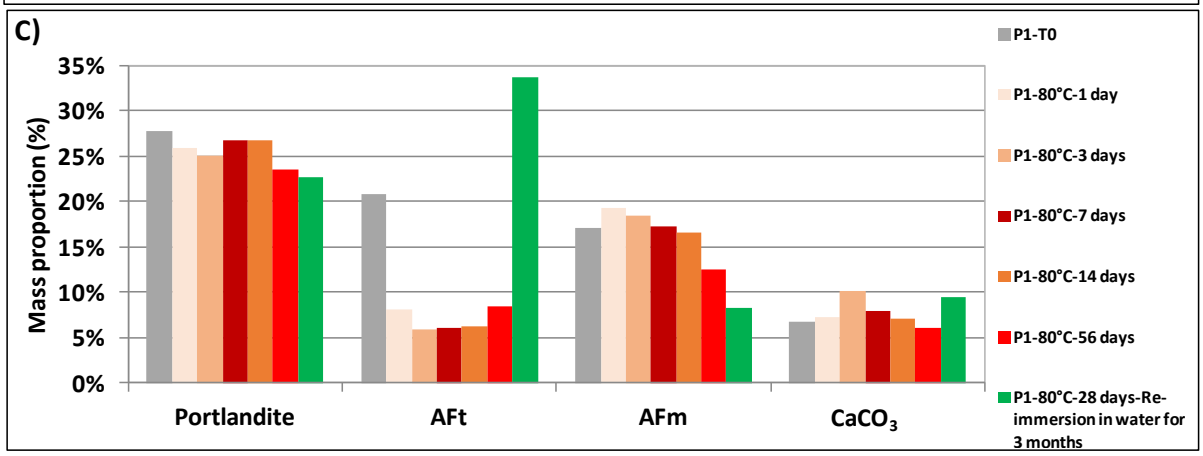
C)
Mass proportion (%)
35%
30%
25%
20%
15%
10%
5%
0%
Portlandite
AFt
AFm
CaCO3
P1-T0
P1-80°C-1 day
P1-80°C-3 days
P1-80°C-7 days
P1-80°C-14 days
P1-80°C-56 days
P1-80°C-28 days-Re-immersion in water for 3 months

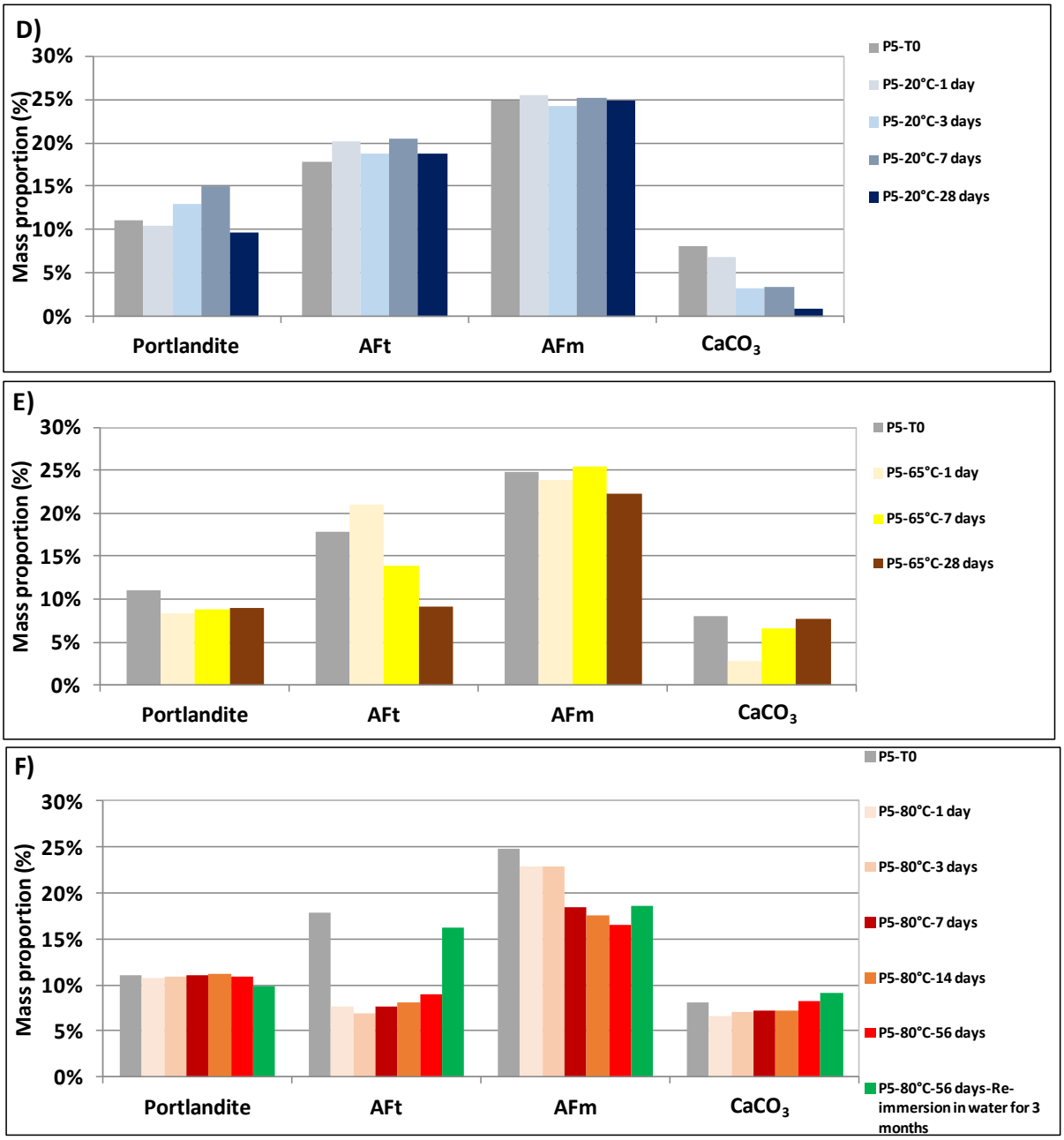

Figure 4. Evolution of the phase assemblage as a function of the TT obtained by the combined method for samples P1 and P5. The mass proportion of the phase is reported to the quantity of the anhydrous.

3.2.2 Equilibrium of aluminate phases

Unlike the thermal treated samples, when samples P1, P2 and P5 were left in a temperature of 20 °C (climatic chamber), only minor modifications were observed for the phase assemblage (e.g. Figure 3A and Figure 3B). These minor modifications were also related to the samples preparation protocol (grinding) as well as the precisions of each experimental technique.

The thermal stability of aluminate phases has been widely studied in literature [19,20,49–58], especially the stability of ettringite at high temperature known as one of the most sensitive phases to the temperature rise. It usually becomes less stable for temperatures above 50 °C or 60 °C in hydrated OPC and blended cement systems [19,20,53–58].
Initially, the quantity of the formed ettringite in samples P1 and P2 was higher compared to sample P5, due to the higher initial ratios of CO_2/Al_2O_3 and SO_3/Al_2O_3 in P1 and P2 than in P5 [59–61].

The ettringite became unstable during TT for temperatures above 65 °C for all cement pastes, according to previous studies [19,20,53–58]. XRD data (see Figure 3) showed that the quantity of ettringite in the system decreased drastically from the very first day of the TT and disappeared after a few days, depending on the used heating temperature. This result was in accordance with the combined method data (see Figure 4) and using the ^{27}Al NMR results (see Figure 5), where the AFt phase proportion decreased during the TT. However, AFt phase did not disappear completely even after 56 days of TT at 80 °C unlike the cristallised ettringite detected by the XRD method. At first sight, this was related to the loss of the crystallinity in the ettringite during the temperature rise due to the lost of its water. This lost made ettringite undetectable using the XRD technique but detectable using the ^{27}Al NMR which focuses on immediate environment of Al. Assuming AFt was composed only by ettringite, the calculations showed that the initial quantity of sulfate available in the system was not enough to satisfy this assumption (4.0% of SO_3 in P1, 3.8% in P2 and 4.6% in P5 was needed). Consequently, the AFt phase was not compound only of ettringite but probably of other tri-substituted aluminate phases (poor in sulfate). Indeed, many publications discussed the possibility of forming C-AFt [56,62,63] phase or Si-AFt phase known as thaumasite [56]. According to [62,63], the C-AFt phase is only possible to be achieved in solution with sucrose as well as sodium carbonate. This phase is not likely to be formed in cement paste due to the greater stability of monocarboaluminate (Mc) [54]. Moreover, both C-AFt and thaumasite are metastable phases at high temperatures [56,64]. Nevertheless, many thermodynamic studies showed that a non-ideal solid solution including both sulfate and carbonate can be stabilized [56,63,65] and 50% to 60% of sulfate could be replaced by carbonate in the AFt phase. Hence, the solid solution was more likely to form the stabilized-AFt at high temperatures in our systems. Additional SEM-EDX measurements could be conducted in order to confirm this hypothesis. The carbonate forming the solid solution can be either coming from the initial proportion of limestone added to the cement in the case of samples P1 and P2 [66], from the initially present impurities in the gypsum [66], or brought by air [66] as the carbonation was promoted in our TT conditions [67].

In addition, the proportion of AFm phases was also changed during the TT. For shorter heating duration or lower temperature (65 °C and 80 °C at 1 day), the AFm proportion increased for both P1 and P2 samples, then decreased for harsher TT (80 °C more than 1 day). For the P5 sample, the AFm proportion diminished during the TT. The XRD was the determining technique to understand the modifications in the AFm phases. The P1 and P2 samples initially formed more AFm-carboaluminate phases (Mc and Hc) compared to P5 (see Figure 3), as their anhydrous cement originally contained more limestone (see Table 3) [59,61]. During the TT, since free sulfates (released by the ettringite) increased the sulfate molarity, this allowed a reducing of Mc and Hc proportion and an increasing of the monosulfoaluminate (Ms) proportion [59,61] (see Kuzelite on Figure 3 and XDR patterns on appendix B, which is the natural analog of Ms in a specific hydration state (n=12) [68]). In the long term of TT, Ms as well as a potentially existent hydroxide-AFm solid solution were metastable at high temperature [56,69], which led to a decreasing of the AFm proportion. The released AFm-sulfates allowed to stabilize more AFt solid solution as it will be shown later (see Figure 11). Finally, the hydrogarnet phase (also called Katoite) partially detectable by XRD became slightly stable as the temperature rose. This phase becomes stable at high temperatures according studies [20,27,70–73]. In the present study, only the Si-free form of Hydrogarnet was detected. In fact, the siliceous hydrogarnet can be only detected for temperatures higher than 100 °C [74,75].
For all P5 samples, the used binder was a cement with a lower sulfate and carbonate content in comparison to its aluminates content (see Table 1 and Table 3). The AFm phase had initially less carboaluminate-AFm phase and more Ms, (see Figure 3 and B.1). A broad peak at 13° (2 theta) was observed on the XRD patterns which corresponded to a solid solution of Mc and Hc. A contribution to this peak could also be hydrotalcite as observed for cement pastes with slag in other studies [76] and was confirmed by our results (see Figure 3). Moreover, it was an aluminate-rich cement containing fly ash. As the consequence, this sample initially formed calcium aluminate hydrates such as hydrated calcium aluminates, hydrogarnet (Katoite) or TAH observed by NMR ^{27}Al (see Figure 5)

[61,77–79]. Unlike the monocarboaluminate, these phases could be able to persist to higher sulfate molarity [27,30,80], which prevented the formation of the Ms at lower TT temperature or at shorter TT duration. After a long TT, the AFm-phase content decreased as the Mc and the Ms became unstable. In addition, the hydrogarnet as well as the hydrotalcite became slightly stable as the temperature increased. The TAH proportion was higher with TT for sample P5 (see Figure 5). This increase was attributed to the formation of hydrotalcite as its peak was superposed with the TAH peak on the ^{27}Al NMR spectra.

Eventually, the total proportion of AFm phases detected by XRD (sum of Mc, Hc, …) was significantly lower to the one detected by ^{27}Al NMR. Low crystallinity of the AFm phases made it only partially detectable by the XRD technique [61]. Indeed, the AFm phase has proven a difficult subject for analysis both because of its low crystallinity, polytypism and because of variations in composition (solid solutions) with corresponding changes to the position and intensity of reflections in its diffraction patterns [61]. Moreover, in blended cements such as slag cement, aluminosilicate-AFm can also be formed [61]. As the result, equilibrium of these phases is more complex for these materials and in particular here with a CEM V/A.

It can be concluded at this level that the AFt phase was a compound of ettringite but also of an expansive (i.e., that may lead to observe swellings in the system afterwards) solid solution of carbonate and sulfate. The variations in the AFm proportions during the TT depended on the initial cement chemistry. However, for all the samples studied here, the equilibriums showed that during the TT, both AFm and AFt were partially destabilized and losing their aluminates. These aluminates were mainly either consumed to form more C-(A)-S-H as mentioned by [81,82], or consumed to form poorly crystallized phases as TAH. Consequently, modifications of C-(A)-S-H were studied in the following section as well as the equilibrium of this one with portlandite and calcite.

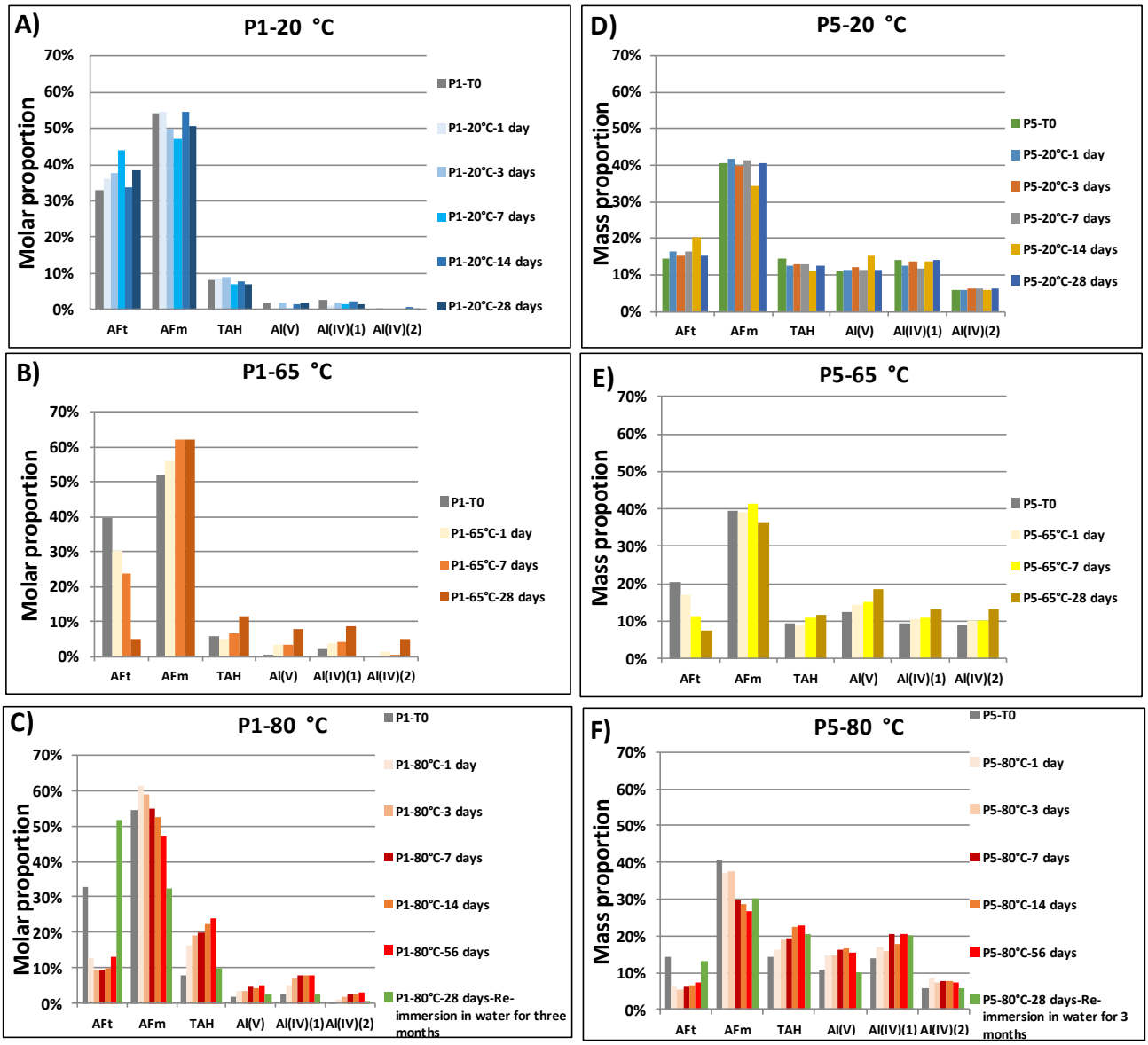

Figure 5. Molar proportion (%) of Al species obtained by ^{27}Al NMR in samples P1 and P5 during the TT. Al(V) and Al(IV): Al substituted to Si or Ca in C-(A)-S-H or alumina gel. Al(IV)(2): Al supposed to be in C_3A.

3.2.3 Portlandite, calcite and C-(A)-S-H

Before the TT, sample P5 contained less portlandite than samples P1 and P2, as it was made with less clinker and more SCMs [29]. During the TT (see Figure 3 and 4), a similar tendency was observed for the portlandite and calcite phases for results obtained by both XRD and combined method. Their proportions were marginally affected by the temperature increase, according to previous studies [17,20,86,87]. On one hand, the observed fluctuations in the portlandite amount were explained by the competition between two phenomena. The increase of portlandite by consuming the released calcium from ettringite was opposed to its reduction caused by the carbonation of the sample. On the other hand, the observed fluctuations in the calcite amount were explained either by the external carbonation of the portlandite which was accelerated in our TT conditions [67], or at a lower level by consuming carbonate and calcium from the destabilized ettringite and carboaluminate-AFm phases. The measured calcite proportion depended on the preparation of each sample, as they were ground before TGA, XRD and NMR measurements. As the consequence, powder of the sample was exposed to natural carbonation, despite the precautions taken to limit this phenomenon.

For C-(A)-S-H, the XRD results showed that the amount of amorphous decreased slightly at 65 °C as well as at 80 °C (not figured here). However, it should be kept in mind that all amorphous in the system was assumed to be C-(A)-S-H. It has to be taken with caution since the system contained other amorphous materials such as alumina gel. Hence, the combined method was more suitable to describe the C-(A)-S-H evolution during the TT. In fact, the characterization was more detailed concerning the repartition of silica in anhydrous and hydrates since it was based on the ^{29}Si NMR technique (see Figure 6 and figure 7).
For all the samples (see Figure 7A and 7B), the TT induced the polymerization of C-(A)-S-H, illustrated here by a higher amount of the Q^3 and Q^4 species (structure similar to silica gel) and a lower amount of Q^1 and Q^2 species (representing C-(A)-S-H chains). Similarly to literature [88], in samples P1 and P2, the polymerization was higher for a soft TT (65 °C) than for a harsher TT (80 °C).
The C-(A)-S-H polymerization was usually observed in literature when the carbonation process was involved leading to the decalcification of C-(A)-S-H [89,90]. However, the polymerization here was induced mainly by the effect of the temperature rise. In this case, a slight decrease of the C/S ratio in the C-(A)-S-H was mentioned in literature [28,91]. This explained the minor modifications in the C/S ratio in the C-(A)-S-H (see Figure 8). In order to estimate the C/S ratio in C-(A)-S-H, it was assumed that the released calcium from ettringite that was not consumed by any other phase (AFm, portlandite or calcite) was only adsorbed on the C-(A)-S-H surface and did not increase its stoichiometric formulae. It was admitted that the calculated C/S ratio in the C-(A)-S-H was relatively low for the P5 sample in comparison with results in literature, this was due to the assumed hydration kinetics of silica and carbonate of the slag in the CEM V. Nevertheless, the trend of the variation of the C/S ratio in the samples regarding the TT was indeed well described by the method. Furthermore, the polymerized C-(A)-S-H was expected to be denser as shown by previous studies [28, 93] and with a higher affinity with sulfate [92]. Moreover, it is worth mentioning that the polymerization may lead to enhance the hydration rate of the samples [93].

On the other hand, for sample P1, the water content in the C-(A)-S-H was also modified during the TT (see Figure 9). For a soft TT (first days at 65 °C), the water content of C-(A)-S-H increased. It was probably adsorbing the free porosity water or the released water from the deteriorated ettringite. When the TT became harsher, the C-(A)-S-H also lost partially its water. This was induced by the effect of the low relative humidity applied during the TT (loss of water molecules between the C-(A)-S-H layers) [94], by the high temperature (loss of water between the C-(A)-S-H layer as well as the OH- groups) [94], but also by the polymerization effect (loss of silanol groups) [92]. A lower water content may lead to a lower hydration rate. Consequently, the competition between the water loss and the polymerization was responsible for the non-monotonous observed variations in the C-(A)-S-H mass proportion.
It was shown above that both AFt and AFm phases (rich in sulfate content) were subject to degradation during the TT (see Section 3.2.2), which led to the question of the prospect of the free released sulfates. Many publications discussed the potential adsorption of the sulfates on the C-(A)-S-H called physical binding [38,59,81,83–85]. According to these researches, the amount of the sulfates binding depends on the C/S ratio in the C-(A)-S-H as well as the temperature [38,85]. In the present study, calculations showed that, even by assuming that all the AFm phase was compound only of Ms (1 sulfate per molecule), no matter the sample, and for the two heating temperatures used here, the Ms content (quantified by ^{27}Al NMR) in the system was not enough to consume all the sulfates released by the ettringite (3 sulfates per molecule) after 7 days of TT. This calculation confirmed that the released sulfates in these systems were free and were probably adsorbed on the C-(A)-S-H surface. Values varying from 0.013 to 0.080 mole of sulfate adsorbed per mole of C-(A)-S-H were measured in previous studies [38,85]. Given the quantity of the C-(A)-S-H in our system, although accepting that the adsorption rate was 0.100 mole SO_3/mole C-(A)-S-H, the C-(A)-S-H was only able to bind partially the released sulfates. However, modifications of the C-(A)-S-H structure during the TT (such as the polymerisation or formation of C-(A)-S-H) that occurred, also influenced

the ability of C-(A)-S-H of sulfates binding [93]. Finally, a part of the non-bound sulfates was used to form the thermo-stable AFt phase as said in section 3.2.2, while the rest probably remained in the interstitial fluid as discussed in previous studies [18,20]. Nevertheless, this interstitial fluid was low since the RH used during TT.

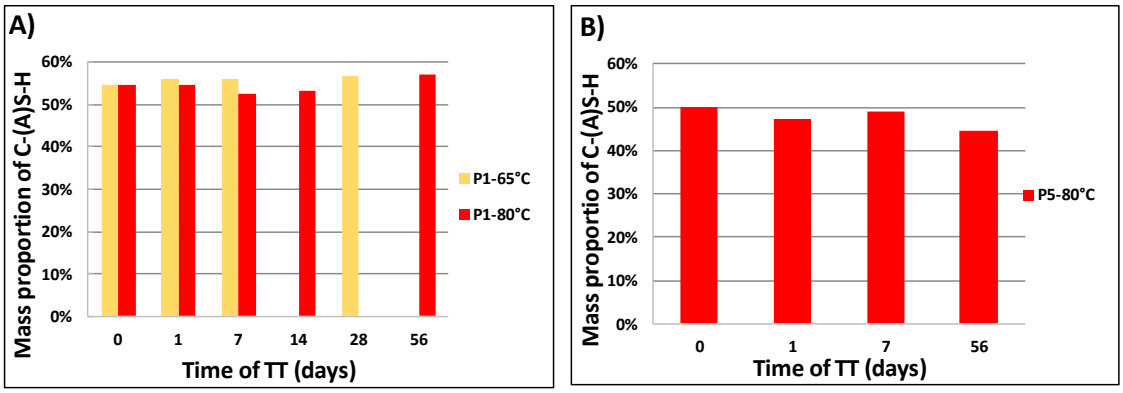

Figure 6. Mass proportion of C-(A)-S-H in cement pastes (P1 and P5), obtained by the combined method [29] as a function of the TT conditions.

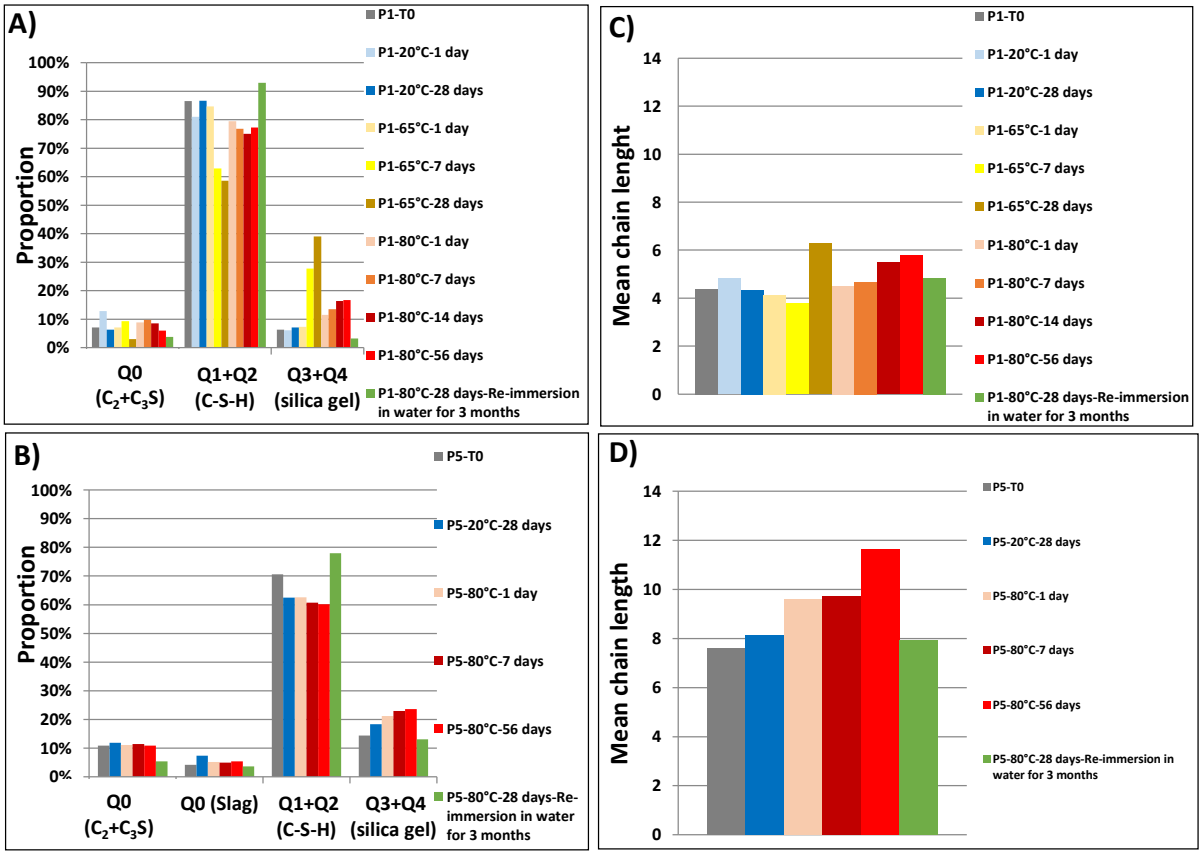

Figure 7. Polymerization of C-(A)-S-H and silica chain length in samples P1 and P5 as a function of the applied TT obtained by ^{29}Si NMR.

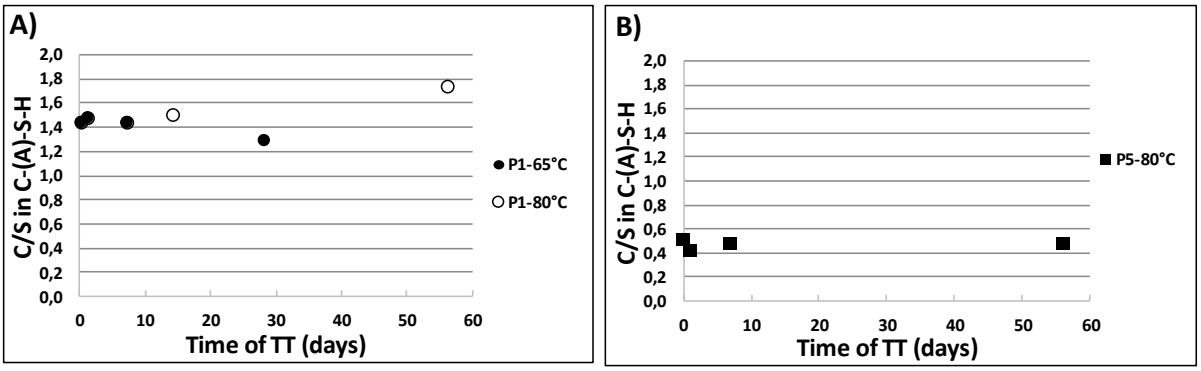

Figure 8. Variations of the C/S ratio in the C-(A)-S-H for cement pastes (P1 and P5) during the TT obtained by the combined method [29].

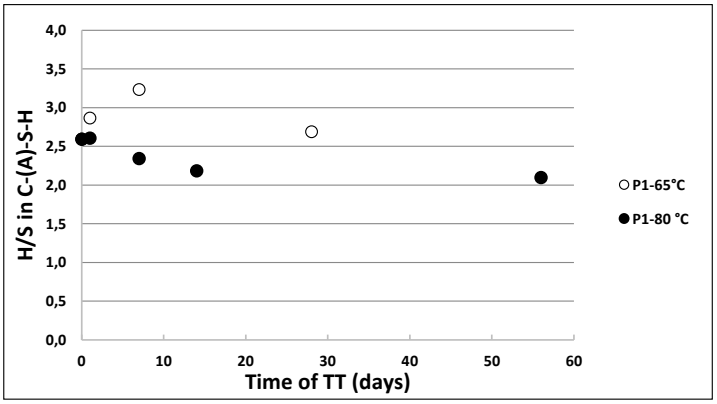

Figure 9. Variations of the H/S ratio in the C-(A)-S-H for P1 cement pastes as function of time of TT at 65 °C and 80 °C obtained by the combined method [29].

3.2 Coupled effect of temperature and duration

Based on results given in Figure 3 and Figure 4, the harsher the TT was (i.e., higher temperature or longer TT), the stronger the assemblage modifications were. The harsh TT conditions probably induced a kinetic accelerating effect of the observed phenomena. Several means were suggested in literature to describe the coupled effect of time and temperature regarding a temperature increase in concrete [81,82,95,96]. The effective thermal energy, which is the product of the heating time and the effective temperature enabled author [81] to describe the combined effect of time and temperature degree on the AFt dissolution. The effective temperature referred here to the elevation of temperature regarding the one from which assemblage modifications occurred in the system (noted T_0), given by the equation (1).

$$UE=\begin{cases}\int (T(t)-T_0)dt & if\ T(t)>T_0 \\ 0 & Otherwise\end{cases} \quad \text{(Eq.1)}$$

The variations of the H/S in the C-(A)-S-H for P1 were obtained as a function of the effective thermal energy (see Figure 10), as the dissolution rate of AFt and AFm in P1 and P5 for a heat rise at 65 °C and 80 °C, and as a function of the effective thermal energy (see Figure 11). Therefore, the dissolution rate of AFm and AFt as well as the drying rate of the C-(A)-S-H were well captured by the effective thermal energy applied during the TT. This proved the earlier suggested assumption that a higher temperature degree or a longer TT accelerated the kinetics of observed phenomena. In addition, it proved that at the thermodynamic equilibrium, the 65 °C results were similar to the 80 °C ones. Finally, the reference temperature (T_0) estimated for the P1 and P2 samples was of the order of 64.5 °C and the one for the P5 was at 64.0 °C. These temperatures were estimated by fitting and therefore

the correlation for the AFt could be obtained. The collected values of T_0 were close to the ones mentioned in literature [81].

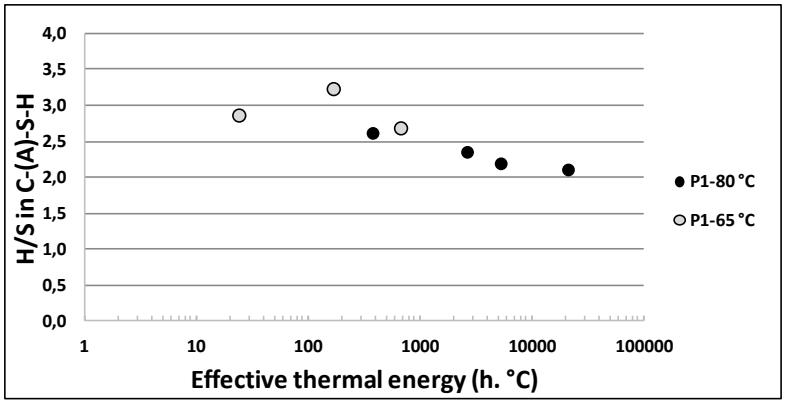

Figure 10. Variations of the H/S ratio (obtained by the combined method [29]) in the C-(A)-S-H for P1 cement paste as function of the effective thermal energy.

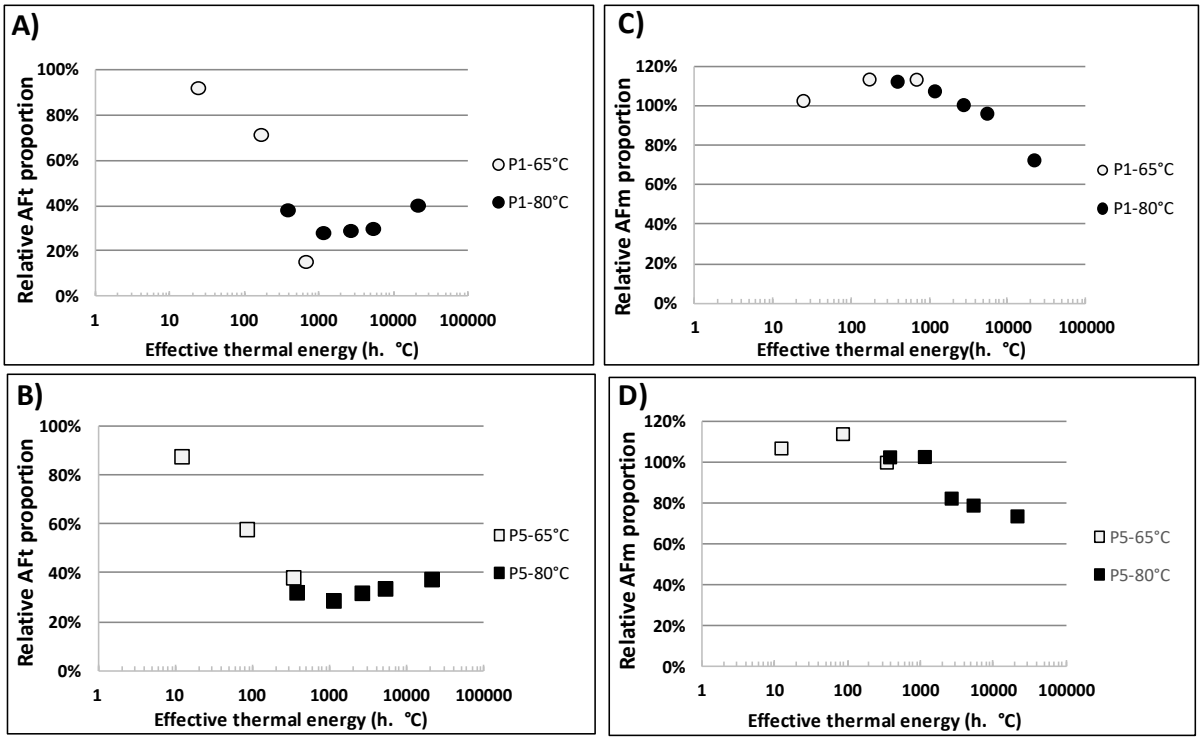

Figure 11. Relative variations of the AFm and AFt content (obtained by ^{27}Al NMR) in cements pastes (P1 and P5) as function of the effective thermal energy.

3.4 Consequences of the temperature rise on the DEF risk (experiences of re-immersion after TT)

In order to observe the DEF after a temperature rise, a relative humidity higher than 92% [97] or 98% [98] is needed. Moreover, the recrystallisation of the expansive AFt phase may be time consuming, depending on the water availability and leaching of alkalis [98]. Thus, the thermal treated samples at 80 °C for 56 days were re-immersed in water for 3 months in order to characterize afterwards the assemblage modifications, linked to the DEF risk.

In all the TT samples (P1 and P5), almost the same quantity of ettringite, presented in the system before the TT, was formed again after the re-immersion of samples in water (see XRD results in figure 3). This was confirmed by the combined method results (see Figure 4). The AFt proportion became

higher than the initially formed AFt proportion for P1 (from 33% to 52%) and P2 (from 35% to 49%), while it stayed similar for P5. As said in section 3.2.2, the AFt phase was a compound of ettringite but also probably of a non-ideal solid solution containing both sulfates and carbonates as well as aluminates. By calculations, the initial solid solution formed in P1 and P2 was more likely to contain 2 molecules of sulfate for each molecule of carbonate. As to the formed solid solution after the TT and the re-immersion in water, it was more likely to contain 1 molecule of sulfate for each 2 molecules of carbonate. The quantity of sulfate was the limiting component. Comparing samples just after TT, the higher production rate of AFt for P1 and P2 after re-immersion was explained by their high SO_3/Al_2O_3 and CO_2/Al_2O_3 ratios, which became even higher because of the lower free aluminates after hydration as well as the carbonation of the samples [59,61]. On the contrary, the P5 sample was more likely to form stable AFm phases (Ms, Hc and hydrogarnet) as well TAH or hydrotalcite.

Besides, the portlandite content in P5 significantly decreased after re-immersion in water (see Figure 4F), meanwhile the calcite content increased significantly in comparison with the results of the TT at 20 °C. As the result, the carbonation in this sample didn't lead to form the AFt solid solution, but led to the carbonation of the portlandite instead.
The AFm phase decreased in P1 and P2 (see ^{27}Al NMR results in Figure 5), while it slightly increased for P5. However, for the latter, it was still lower than the AFm proportion in the reference sample (before TT). In addition, the content of crystallized aluminate phases (Ms, Hc and Mc) became higher after re-immersion comparing the sample just after the TT (see XRD results in Figure 3) but they were still lower than the ones of reference samples. A part of silica-free Hydrogarnet (formed during the TT) was stabilized in the cement paste after re-immersion. This re-immersion induced a re-crystallization effect of the AFm phases. Nonetheless, the question whether the total quantity of Mc, Ms or Hc including both amorphous and crystallized phases (observed by ^{27}Al NMR) would have effectively increase after re-immersion. For P5, the crystallized Ms and Mc proportions became equal or even higher after re-immersion comparing to the ones of reference samples (see XRD results in Figure 3F). The Hc did not form after re-immersion. Finally, a non-neglectable part of the formed silica-free hydrogarnet during the TT was obviously stabilized after re-immersion. It was in accordance with the NMR ^{27}Al results (see Figure 5F). In fact, the AFm proportion increased regarding the one of sample just after the TT. Moreover, the increase of hydrotalcite (whose peak was superposed with the TAH peak in ^{27}Al NMR spectra) was irreversible in P5 while, on the contrary, it was reversible in P1 and P2 after a cycle of TT and re-immersion.
It can be concluded at this level that the P5 sample was more able to stabilize the AFm and hydrotalcite phases (Ms, hydrogarnet and hydrotalcite), unlike the P1 and P2 ones which were more able to stabilize the AFt phase. This was due to the presence of slag in the cement according previous study [76] as well as its low sulfate and carbonate content [59,61]. Furthermore, both hydrogarnet and hydrotalcite were formed irreversibly (at least for a re-immersion time of 91 days). As seen in a previous study [80], they did not release their aluminates to react with the free sulfates, which affected the free aluminates content.
There are traditional ways to analyze the expansion probability based only on the sulfate and aluminates content as suggested by literature [5,99]. Contrary to the previously used method developed in another study [61], these methods only relied on the sulfates on aluminates ratio, and did not take into account neither the carbonate content in the system nor the slag content. Based on our calculations, the SO_3/Al_2O_3 ratio was of the order of 0.65 and 0.60 respectively for P1 and P2 and only of the order of 0.30 for the cement paste P5 before the TT. Consequently, P1 and P2 initially formed ettringite as confirmed by the XRD and the combined method. After the TT and re-immersion, the free aluminates proportion available to form the AFt phase was mainly modified due to the thermodynamically stable hydrogarnet and hydrotalcite. In fact, it was noted through the NMR ^{27}Al results that the aluminates adsorption on the C-(A)-S-H was almost completely reversible especially for P1 and P2. Moreover, a part of the aluminates was initially consumed to form the TAH and C-(A)-S-H, this non-thermal-treatment-related formation of C-(A)-S-H was irreversible according to the ^{27}Al NMR results. In addition, it also induced a decrease in the available free aluminates in the

system. The consumed aluminates by silica-free hydrogarnet during the TT was hard to quantify given the low crystallinity degree of the AFm phases. As the result, it was considered here the consumed aluminates by the non-thermal-treatment-related formed C-(A)-S-H as well as the irreversibly formed TAH which was attributed to hydrotalcite. Even in this case, the SO_3/Al_2O_3 ratio increased to 0.75 for both P1 and P2, and it was only of the order of 0.60 for P5. Here, it was assumed that the adsorption of the sulfate on the C-(A)-S-H was almost totally reversible as shown in a previous study [13]. A second assumption was that a possible equilibrium between the AFt and AFm phase may occur which led to consider all sulfates of AFm phase as free sulfates. These results explained the higher ability of forming expansive AFt phases in P1 and P2 as the SO_3/Al_2O_3 ratio was at the critical value of 0.75 [99]. However, it should be admitted that at the same SO_3/Al_2O_3 ratio, the total quantity of the formed ettringite depended on the sulfate quantity, which affected the DEF probability also depending on the porosity network of the system. Consequently, in our case, P5 samples had less ability to develop a DEF pathology afterwards than P1 or P2.
Regarding the C-(A)-S-H modifications after re-immersion, the polymerization effect (induced by the TT) was almost completely reversible (see Figure 7). The silicate chain length became shorter and the Q^1 and Q^2 C-(A)-S-H proportions appeared higher after re-immersion. Moreover, as samples were left for additional 3 months in water which promoted further their hydration rate, the C/S in C-(A)-S-H became slightly higher after re-immersion in water. C/S in C-(A)-S-H was equal to 1.60 for P1, 1.54 for P2 and 0.60 for P5.
Finally, an expansion pessimism effect was mentioned in literature [15,39,81]. In fact, a TT duration from which the temperature rise no longer induced an increase in the expansion amplitude. It showed an effect of curing the sample since a longer TT led the expansion amplitude to decrease. Values between 2 and 14 days were affected to the critical pessimism duration in literature [39,81]. In a previous study [39], this effect was explained by an irreversible adsorption of aluminates on the C-(A)-S-H during the TT, which inferred a decrease of the available aluminates. In another study [81], it was explained by the irreversible formation of the siliceous hydrogarnet during the TT which also led to the decrease of the quantity of the available aluminates. Nevertheless, our results showed a sudden increase of the Al_2O_3 /SiO_2 ratio in the C-(A)-S-H once the decomposition of ettringite occurred as also shown in literature [30]. In addition, the phenomenon was almost completely reversible after the temperature drop and re-immersion in water. Furthermore, the hydrogarnet was formed in aluminates rich cements with low sulfates and carbonate content, while the pessimism effect seemed to be found in other cement types. In this work, an irreversible formation of a non-ideal AFt solid solution occurred in the system after 3 to 7 days of TT. This AFt formation led to the consumption of aluminates and a decrease of the free aluminates available to, then, form the expansive AFt phase after re-immersion, which can indeed explain the pessimism effect.

4 Conclusion

In this paper, the effects of a delayed heating applied on various hydrated cement pastes (CEM I, CEM II/A and CEM V/A) on the phase assemblage were studied. The samples were kept for at least 400 days under water before the TT was applied. Two heating temperatures (65 °C and 80 °C) were applied for durations between 1 day and 56 days, and the results were compared to samples kept at a temperature of 20 °C (climatic chamber). The relative humidity of all treatments was 55% for all samples.
For all samples, the ettringite was destabilized since the first day of the temperature rises. However, the AFm and AFt modifications depended on the mineralogy of each hydrated cement. For P1 and P2, since they were designed using cements with high SO_3/Al_2O_3 and CO_2/Al_2O_3, they stabilized AFt phases before the temperature rise as well as after cooling, and more AFm phases (Ms and Mc) during the TT. As the aluminates-rich sample P5, it was more likely to form the thermodynamically stable AFm phases such as hydrogarnet as well as hydrotalcite. It influenced the free elements available after cooling and led to form less the expansive AFt phase in P5 in comparison with P1 and P2. Moreover, it was shown that no matter the sample, the same quantity of ettringite was present

in the system before the TT crystallized again after cooling and re-immersion in water for 91 days. However, only the non-ideal AFt solid solution was influenced by the cement chemistry. This solid solution was a compound of sulfate and carbonate and were responsible for the expansions related to the DEF. In addition, a slight proportion of AFt was stabilized after several days of TT, which explained the expansions pessimism effect discussed in literature. Furthermore, modification in C-(A)-S-H during the TT were studied. The C/S ratio in the C-(A)-S-H was almost constant during the TT while the C-(A)-S-H chains became longer and their aluminate content appeared higher. Finally, it was shown that the elevation of temperature and/or duration induced an accelerating effect of the variations in the aluminate phases and the drying effects according to the concept of effective thermal energy.

After the temperature drop and re-immersion in water for 3 months, the majority of the TT-related phenomena seemed to be reversible. The aluminates adsorbed on the C-(A)-S-H were almost completely desadsorbed and the polymerization degree of C-(A)-S-H decreased. Only the formation of the thermodynamically stable phases formed mainly in P5 (Hydrotalcite and hydrogarnet) was an irreversible phenomenon. Modifications in the free aluminates content, as well as the carbonation, led to the SO_3/Al_2O_3 and the CO_2/Al_2O_3 ratios became even higher in the P1 and P2 samples, which boosted further their ability to form the expansive AFt phases unlike in the P5 sample. Consequently, DEF risk is more probable in case of P1 and P2 rather than in case of P5. This will be verified in the future study on expansion of concretes exposed to heat treatment.

Acknowledgements

The authors are grateful to Jean-Baptiste d'Espinose de Lacaillerie (ESPCI-Paris) for NMR experiments, to Raphaëlle Prié for the work done during her a three-month internship on this project and to C. Couffe for the English proofreading of this article.

References

[1] L. Divet, F. Guerrier, G. Le Mertre, Is there a risk of endogenous sulphate attack in high mass concrete members? The example of the pont Ondes (Haute-Garonne), Bulletin des Laboratoires des Ponts et Chaussées 213 (1998) 59-72.

[2] S. Lagundzija, M. Thiam, Temperature reduction during concrete hydration in massive structures, KTH, Sweden. 2017. Corpus ID: 202943691.

[3] N. Aniskin, N.C. Chyk, Temperature regime of massive concrete dams in the zone of contact with the base, IOP Conference Series: Materials Science and Engineering 365 (2018), IOP Publishing. https://doi.org/10.1088/1757-899X/365/4/042083

[4] I.A. Korotchenko, E.N. Ivanov, S.S. Manovitsky, V.A. Borisova, K.V. Semenov, Y.G. Barabanshchikov, Deformation of concrete creep in the thermal stress state calculation of massive concrete and reinforced concrete structures, Magazine of Civil Engineering 69 (2017) 56-63. https://doi.org/10.18720/MCE.69.5

[5] J.M. Torrenti, Basic creep of concrete-coupling between high stresses and elevated temperatures, European Journal of Environmental and Civil Engineering, 22 (2018) 1419-1428. https://doi.org/10.1080/19648189.2017.1280417

[6] F. Acosta Urrea, Influence of elevated temperatures up to 100° C on the mechanical properties of concrete, KIT Scientific Publishing, HEFT 84, 2018.

[7] D. Heinz, U. Ludwig, Mechanism of secondary ettringite formation in mortars and concretes subjected to heat treatment, Special Publication 100 (1987) 2059-2072.

[8] C.D. Lawrence, Mortar expansions due to delayed ettringite formation. Effects of curing period and temperature, Cement and concrete research, 25 (1998) 903-914. https://doi.org/10.1016/0008-8846(95)00081-M

[9] K.L. Scrivener, D. Damidot, C. Famy, Possible mechanisms of expansion of concrete exposed to elevated temperatures during curing (also known as DEF) and implications for avoidance of field problems, Cement, Concrete and Aggregates 21 (1999) 93-101.
[10] N. Petrov, A. Tagnit-Hamou, Is microcracking really a precursor to delayed ettringite formation and consequent expansion?, Materials Journal 101 (2004) 442-447.
[11] R. Barbarulo, H. Peycelon, S. Prené, J. Marchand, Delayed ettringite formation symptoms on mortars induced by high temperature due to cement heat of hydration or late thermal cycle, Cement and concrete research 35 (2005) 125-131. https://doi.org/10.1016/j.cemconres.2004.05.041
[12] R.P. Martin, C. Bazin, J. Billo, M. Estivin, J.C. Renaud, F. Toutlemonde, , Experimental evidence for understanding DEF sensitivity to early-age thermal history, RILEM-JCI International Workshop on Crack Control of Mass Concrete and Related Issues Concerning Early-Age of Concrete Structures, (2012) 0-10.
[13] L. Divet, Internal sulfate reactions in concrete: contribution to the study of the mechanisms of the delayed ettringite formation, Etudes et Recherches des Laboratoires des Ponts et Chaussées, Série Ouvrages d'Art, OA 40 (2001). *In french*
[14] K.L. Scrivener, H.F.W. Taylor, Delayed ettringite formation: a microstructural and microanalytical study, Advances in Cement Research 20 (1993), 139-146. https://doi.org/10.1680/adcr.1993.5.20.139
[15] H.F.W. Taylor, C. Famy K.L. Scrivener, Delayed ettringite formation, Cement and Concrete Research 31 (2001) 683-693. https://doi.org/10.1016/S0008-8846(01)00466-5
[16] C. Famy, Expansion of heat-cured mortars, PhD Thesis, Imperial College London, UK, 1999.
[17] J.I. Escalante-Garcia, J.H. Sharp, Effect of temperature on the hydration of the main clinker phases in Portland cements: Part I, neat cements, Cement and concrete research 28 (1998) 1245-1257. https://doi.org/10.1016/S0008-8846(98)00115-X
[18] K.O. Kjellsen, R.J. Detwiler, O.E. Gjørv, Development of microstructures in plain cement pastes hydrated at different temperatures, Cement and concrete research 21 (1991) 179-189. https://doi.org/10.1016/0008-8846(91)90044-I
[19] B. Lothenbach, F. Winnefeld, C. Alder, E. Wieland, P. Lunk, Effect of temperature on the pore solution, microstructure and hydration products of Portland cement pastes, Cement and Concrete Research 37 (2007) 483-491. https://doi.org/10.1016/j.cemconres.2006.11.016 https://doi.org/10.1016/j.cemconres.2006.11.016
[20] B. Lothenbach, T. Matschei, G. Möschner, F.P. Glasser, Thermodynamic modelling of the effect of temperature on the hydration and porosity of Portland cement, Cement and Concrete Research 38(2008) 1-18. https://doi.org/10.1016/j.cemconres.2007.08.017
[21] K.O. Kjellsen, R.J. Detwiler, O.E. Gjørv, Backscattered electron imaging of cement pastes hydrated at different temperatures, Cement and concrete research 20 (1990) 308-311. https://doi.org/10.1016/0008-8846(90)90085-C
[22] K.O. Kjellsen, R.J. Detwiler, O.E. Gjørv, Pore structure of plain cement pastes hydrated at different temperatures, Cement and concrete research 20 (1990) 927-933. https://doi.org/10.1016/0008-8846(90)90055-3
[23] K.O. Kjellsen, R.J. Detwiler, Reaction kinetics of Portland cement mortars hydrated at different temperatures, Cement and Concrete Research 22 (1992) 112-120. https://doi.org/10.1016/0008-8846(92)90141-H
[24] X. Zhang, Quantitative microstructural characterization of concrete cured under realistic temperature conditions, PhD Thesis THESIS, EPFL, Lausanne, 2007.
[25] X. Pang, W.C. Jimenez, J. Singh, Measuring and modeling cement hydration kinetics at variable temperature conditions, Construction and Building Materials 262 (2020) 120788. https://doi.org/10.1016/j.conbuildmat.2020.120788
[26] X. Pang, L. Sun, F. Sun, G. Zhang, S. Guo, Y. Bu, Cement hydration kinetics study in the temperature range from 15° C to 95° C, Cement and Concrete Research 148 (2021) 106552. https://doi.org/10.1016/j.cemconres.2021.106552
[27] F. Deschner, B. Lothenbach, F. Winnefeld, J. Neubauer, Effect of temperature on the hydration of Portland cement blended with siliceous fly ash, Cement and concrete research 52 (2013) 169-181.
[28] S. Bahafid, S. Ghabezloo, M. Duc, P. Faure, J. Sulem, Effect of the hydration temperature on the microstructure of Class G cement: CSH composition and density, Cement and Concrete Research 95 (2017) 270-281. https://doi.org/10.1016/j.cemconres.2017.02.008
[29] M. Saillio, V. Baroghel-Bouny, M. Bertin, S. Pradelle, J. Vincent, Phase assemblage of cement pastes with SCM at different ages, Construction and Building Materials 224 (2019) 144-157. https://doi.org/10.1016/j.conbuildmat.2019.07.059

[30] D.P. Prentice, B. Walkley, S. Bernal, M. Bankhead, M. Hayes, J.L. Provis, Thermodynamic modelling of BFS-PC cements under temperature conditions relevant to the geological disposal of nuclear wastes, Cement and Concrete Research 119 (2019) 21-35. https://doi.org/10.1016/j.cemconres.2019.02.005
[31] M. Al Shamaa, S. Lavaud, L. Divet, G. Nahas, J.M. Torrenti, Coupling between mechanical and transfer properties and expansion due to DEF in a concrete of a nuclear power plant, Nuclear engineering and design 266 (2014) 70-77. https://doi.org/10.1016/j.nucengdes.2013.10.014
[32] M. Saillio, H. Sabeur, J. Vincent, B. Zitoun, Phase assemblage of a 5 year-old cement paste after submission to various high temperature and cooling regime, Construction and Building Materials 279 (2021) 122440. https://doi.org/10.1016/j.conbuildmat.2021.122440
[33] F.A. Selim, M.S. Amin, M. Ramadan, M.M. Hazem, Effect of elevated temperature and cooling regimes on the compressive strength, microstructure and radiation attenuation of fly ash–cement composites modified with miscellaneous nanoparticles, Construction and Building Materials 258 (2020) 119648. https://doi.org/10.1016/j.conbuildmat.2020.119648
[34] B. Georgali, P.E. Tsakiridis, Microstructure of fire-damaged concrete. A case study, Cement and Concrete composites, 27 (2005) 255-259. https://doi.org/10.1016/j.cemconcomp.2004.02.022
[35] J.C. Mindeguia, H. Carré, P. Pimienta, C. La Borderie, Experimental discussion on the mechanisms behind the fire spalling of concrete, Fire and Materials 39 (2015) 619-635.
[36] M.A. Tantawy, Effect of high temperatures on the microstructure of cement paste, Journal of Materials Science and Chemical Engineering 5 (2017) 33. https://doi.org/10.4236/msce.2017.511004
[37] C. Famy, K.L. Scrivener, A. Atkinson, A.R. Brough, Effects of an early or a late heat treatment on the microstructure and composition of inner CSH products of Portland cement mortars, Cement and Concrete Research 32(2002) 269-278. https://doi.org/10.1016/S0008-8846(01)00670-6
[38] R. Barbarulo, Behavior of cementitious materials: actions of sulfates and temperature, PhD Thesis, LMT-ENS de Cachan, France, 2002. *In french*
[39] X. Brunetaud, Study of the influence of different parameters and their interactions on the kinetics of the amplitude of the internal sulfate reaction in concrete, PhD Thesis, Ecole Centrale Paris, Paris, France, 2005. *In french*
[40] R.P. Martin, C. Bazin, J.C. Renaud, F Toutlemonde, Experimental study of DEF expansions of concrete mixes submitted to early and late heat treatments, 7th international conference on concrete under severe conditions, 2013.
[41] French project for a deep disposal center for radioactive waste, https://www.andra.fr/cigeo, accessed 16/12/2022. *In french*
[42] G. Villain, M. Thiery, G. Platret, Measurement of carbonation profiles in concrete: Thermogravimetry, chemical analysis and gammadensimetry, Cement and Concrete Research 37 (2007) 1182-1192. https://doi.org/10.1016/j.cemconres.2007.04.015
[43] F. Winnefeld, A. Schöler, B. Lothenbach, Sample preparation. A practical guide to microstructural analysis of cementitious materials, (2016) 1-36.
[44] W. Chen, H.J.H. Brouwers, The hydration of slag, part 1: reaction models for alkali-activated slag, Journal of materials science 42 (2007) 428-443. https://doi.org/10.1007/s10853-006-0873-2
[45] G. Engelhardt, D. Michel, High-resolution solid-state NMR of silicates and zeolites, Wiley, New York, USA, 1987.
[46] M. Fleury, T. Chevalier, G. Berthe, W. Dridi, M. Adadji, Water diffusion measurements in cement paste, mortar and concrete using a fast NMR based technique, Construction and Building Materials 259 (2020) 119843. https://doi.org/10.1016/j.conbuildmat.2020.119843
[47] M. Saillio, V. Baroghel-Bouny, Chloride binding in sound and carbonated cementitious materials with various types of binder, Construction and Building Materials 68 (2014) 82-91. https://doi.org/10.1016/j.conbuildmat.2014.05.049
[48] M. Mejdi, W. Wilson, M. Saillio, T. Chaussadent, L. Divet, A. Tagnit-Hamou, Quantifying glass powder reaction in blended-cement pastes with the Rietveld-PONKCS method, Cement and Concrete Research 130 (2020) 105999. https://doi.org/10.1016/j.cemconres.2020.105999
[49] M. Atkins, F.P. Glasser, T.G. Jappy, A. Kindness, L.P. Moroni, M. Constable, C.R. Wilding, Effect of elevated temperature on blended cement in radioactive waste disposal, UK DoE Report, University of Aberdeen, UK, 1991.
[50] T.G. Jappy, F.P. Glasser, Synthesis and stability of silica-substituted hydrogarnet Ca_3Al_2 Si_3-xO_{12}-4x (OH) 4x, Advances in cement research, 4 (1991) 1-8. https://doi.org/10.1680/adcr.1991.4.1.1

[51] M. Atkins, F.P. Glasser, A. Kindness, D.E. Macphee, Solubility data for cement hydrate phases (25 °C) (No. DOE-HMIP-RR--91.032), Department of the Environment, UK, 1991.
[52] C.J. Warren, E.J. Reardon, The solubility of ettringite at 25 °C. Cement and Concrete Research 24 (1994) 1515-1524. https://doi.org/10.1016/0008-8846(94)90166-X
[53] R.B. Perkins, C.D. Palmer, Solubility of ettringite (Ca_6 [Al (OH) $_6$]$_2$ (SO_4)$_3$· 26H_2O) at 5–75° C, Geochimica et Cosmochimica Acta 63(1999) 1969-1980. https://doi.org/10.1016/S0016-7037(99)00078-2
[54] D. Damidot, F.P. Glasser, Thermodynamic investigation of the CaO-Al_2O_3-$CaSO_4$-H_2O system at 25° C and the influence of Na_2O, Cement and concrete research 23 (1993) 221-238. https://doi.org/10.1016/0008-8846(93)90153-Z
[55] D. Damidot, F.P. Glasser, Thermodynamic investigation of the CaO-Al_2O_3-$CaSO_4$-H_2O system at 50° C and 85° C, Cement and Concrete Research 22 (1992) 1179-1191. https://doi.org/10.1016/0008-8846(92)90047-Y
[56] T. Matschei, B. Lothenbach, F.P. Glasser, Thermodynamic properties of Portland cement hydrates in the system CaO–Al_2O_3–SiO_2–$CaSO_4$–$CaCO_3$–H_2O, Cement and Concrete Research 37 (2007) 1379-1410. https://doi.org/10.1016/j.cemconres.2007.06.002.
[57] T. Matschei, F.P. Glasser, Temperature dependence, 0 to 40 °C, of the mineralogy of Portland cement paste in the presence of calcium carbonate, Cement and Concrete Research, 40 (2010), 763-777. https://doi.org/10.1016/j.cemconres.2009.11.010.
[58] D. Damidot, B. Lothenbach, D. Herfort, F.P. Glasser, Thermodynamics and cement science, Cement and Concrete Research 41 (2011) 679–695. https://doi.org/10.1016/j.cemconres.2011.03.018.
[59] T. Matschei, R. Skapa, B. Lothenbach, F.P. Glasser, The distribution of sulfate in hydrated Portland cement paste, Proceedings of the 12th Intern. Congress on the Chemistry of Cements, Montreal, Canada, 2007.
[60] H.J. Kuzel, H. Pöllmann, Hydration of C_3A in the presence of $Ca(OH)_2$,$CaSO_4$·2H_2O and $CaCO_3$, Cement and Concrete Research 21 (1991) 885-895. https://doi.org/10.1016/0008-8846(91)90183-I
[61] T. Matschei, B. Lothenbach, F.P. Glasser, The AFm phase in Portland cement, Cement and Concrete Research 37 (2007) 118-130. https://doi.org/10.1016/j.cemconres.2006.10.010
[62] E.T. Carlson, H.A Berman, Some observations on the calcium aluminate carbonate hydrates, Journal of research of the National Bureau of Standards, Section A, Physics and chemistry 64 (1960), 333.
[63] H. Poellmann, H.J. Kuzel, R. Wenda, Solid solution of ettringites part I: incorporation of OH^- and CO_3^{2-} in 3CaO·Al_2O_3·32H_2O, Cement and Concrete Research 20 (1990) 941–947. https://doi.org/10.1016/0008-8846(90)90057-5
[64] T. Matschei, F.P. Glasser, Thermal stability of thaumasite, Materials and Structures 48(2015) 2277-2289.
[65] S.J. Barnett, C.D. Adam, A.R.W. Jackson, An XRPD profile fitting investigation of the solid solution between ettringite, Ca_6Al_2 (SO_4)$_3$ (OH)$_{12}$· 26H_2O, and carbonate ettringite, $Ca_6Al_2(CO_3)_3(OH)_{12}$· 26$H_2O$, Cement and Concrete Research 31 (2001) 13-17. https://doi.org/10.1016/S0008-8846(00)00429-4
[66] T.I. Barry, F.P. Glasser, Calculations of Portland cement clinkering reactions, Advances in cement research 12 (2000) 19-28. https://doi.org/10.1680/adcr.2000.12.1.19
[67] P. Liu, Y. Chen, Z. Yu, Effects of temperature, relative humidity and carbon dioxide concentration on concrete carbonation, Magazine of Concrete Research 72 (2020) 936-947. https://doi.org/10.1680/jmacr.18.00496
[68] T. Honorio, P. Guerra, A. Bourdot, Molecular simulation of the structure and elastic properties of ettringite and monosulfoaluminate, Cement and Concrete Research 135 (2020) 106126. https://doi.org/10.1016/j.cemconres.2020.106126
[69] H. Poellmann, Solid solution in the system 3CaO.Al_2O_3.$CaSO_4$.aq-3CaO.Al_2O_3.$Ca(OH)_2$.aq-H_2O at 25 °C, 45 °C, 60 °C, 80 °C, Neues Jahrbuch für Mineralogie, Abhandlungen, 161 (1989) 27-40.
[70] N.C. Collier, N.B. Milestone, J. Hill, I.H. Godfrey, Immobilisation of Fe floc: Part 2, encapsulation of floc in composite cement, Journal of nuclear materials 393 (2009) 92-101. https://doi.org/10.1016/j.jnucmat.2009.05.010
[71] G. Le Saout, E. Lécolier, A. Rivereau, H. Zanni, Chemical structure of cement aged at normal and elevated temperatures and pressures: Part I. Class G oilwell cement, Cement and concrete research 36 (2006) 71-78. https://doi.org/10.1016/j.cemconres.2004.09.018
[72] N. Neuville, E. Lécolier, G. Aouad, A. Rivereau, D. Damidot, Effect of curing conditions on oilwell cement paste behaviour during leaching: Experimental and modelling approaches, Comptes Rendus Chimie 12 (2009) 511-520. https://doi.org/10.1016/j.crci.2008.06.006
[73] M. Paul, F.P. Glasser, Impact of prolonged warm (85 °C) moist cure on Portland cement paste, Cement and Concrete Research 30 (2000), 1869-1877. https://doi.org/10.1016/S0008-8846(00)00286-6
[74] E.T. Carlson, Hydrogarnet Formation in the System Lime-AI umina -Silica –Water, Journal of Research of the National Bureau of Standards 56 (1956) 327.

[75] B.Z. Dilnesa, B. Lothenbach, G. Renaudin, A. Wichser, D. Kulik, Synthesis and characterization of hydrogarnet $Ca_3(Al_xFe_{1-x})_2(SiO_4)_y(OH)_{4(3-y)}$, Cement and Concrete Research 59 (2014) 96-111. https://doi.org/10.1016/j.cemconres.2014.02.001
[76] S. Stephant, PhD thesis, Study of the influence of slag hydration on gas transfer properties in cementitious materials, Université de Bourgogne, Dijon, France, 2015. *In french*
[77] C. Giraudeau-Lenain, Organoaluminate interactions in cements: intercalation of polymethacrylates-g-PEO in hydrocalumite, PhD Thesis, Paris 6 University, France, 2009. *In french*
[78] G.K. Sun, J.F. Young, R.J. Kirkpatrick, The role of Al in C–S–H: NMR, XRD, and compositional results for precipitated samples, Cement and Concrete Research 36 (2006) 18-29. https://doi.org/10.1016/j.cemconres.2005.03.002
[79] E. L'Hôpital, B. Lothenbach, G. Le Saout, D. Kulik, K. Scrivener, Incorporation of aluminium in calcium-silicate-hydrates, Cement and Concrete Research 75 (2015) 91-103. https://doi.org/10.1016/j.cemconres.2015.04.007
[80] T. Ramlochan, M.D.A Thomas, R.D. Hooton, The effect of pozzolans and slag on the expansion of mortars cured at elevated temperature: Part II: Microstructural and microchemical investigations, Cement and Concrete Research 34 (2004), 1341-1356. https://doi.org/10.1016/S0008-8846(02)01066-9
[81] B. Kchakech, Study of the influence of the heating undergone by a concrete on the risk of expansions associated with the Internal Sulfatic Reaction, PhD Thesis, Paris Est University, France, 2015. *In french*
[80] M. Salgues, Modeling the structural effects of internal sulfate reactions: application to concrete dams (Doctoral dissertation, PhD Thesis, Université Toulouse III-Paul Sabatier, France, 2013. *In french*
[83]S.A. Gunay, Influence of the hydration kinetics of the aluminate phases in the presence of calcium sulphate on those of the silicate phases: consequences on the optimum sulphation of cements, PhD Thesis, Université de Bourgogne, France, 2012. *In french*
[84] L. Nachbaur. (1997), Study of the mechanism of the Analysis of the addition of electrolytes and polyelectrolytes on the hydration of tricalcium silicate and the fundamental processes of coagulation and rigidification determining the setting, PhD Thesis, Université de Bourgogne, France. *In french*
[85] M. Medala, I. Pochard, C. Labbez, A. Nonat, Investigations of the interacting forces between Calcium Silicate Hydrate (CSH) particles: influence of sulfate ions sorption on CSH, Proceeding of the Cement and Concrete Science Conference, Leeds, UK, (2009) 8-9.
[86] J.J. Thomas, D. Rothstein, H.M. Jennings, B.J. Christensen, Effect of hydration temperature on the solubility behavior of Ca-, S-, Al-, and Si-bearing solid phases in Portland cement pastes, Cement and Concrete Research 33 (2003) 2037-2047. https://doi.org/10.1016/S0008-8846(03)00224-2.
[87] R.J. Myers, E. L'Hôpital, J. Provis, B. Lothenbach, Effect of temperature and aluminium on calcium (alumino) silicate hydrate chemistry under equilibrium conditions, Cement and Concrete Research 68(2015) 83-93. https://doi.org/10.1016/j.cemconres.2014.10.015
[88] Q. Ding, C. Hu, X. Feng, X. Huang, Effect of curing regime on polymerization of CSH in hardened cement pastes, Journal of Wuhan University of Technology-Mater. Sci. Ed. 28 (2013) 715-720. https://doi.org/10.1007/s11595-013-0758-6
[89] A. Morandeau, M. Thiery, P. Dangla, Investigation of the carbonation mechanism of CH and CSH in terms of kinetics, microstructure changes and moisture properties, Cement and Concrete Research 56 (2014) 153-170. https://doi.org/10.1016/j.cemconres.2013.11.015
[90] B. Wu, G. Ye, Carbonation mechanism of different kind of CSH: rate and products. Int. RILEM Conference on Materials, Systems and Structures in Civil Engineering 2016-Segment on Concrete with Supplementary Cementitious Materials (2016) 163-272.
[91] I.G. Richardson, The calcium silicate hydrates, Cement and concrete research 38 (2008) 137-158. https://doi.org/10.1016/j.cemconres.2007.11.005
[92] E. Gallucci, X. Zhang, K. Scrivener, Effect of temperature on the microstructure of calcium silicate hydrate (CSH), Cement and Concrete Research 53 (2013) 185-195. https://doi.org/10.1016/j.cemconres.2013.06.008
[93] J. Haas, Experimental study and thermodynamic modeling of the CaO-SiO_2-(Al_2O_3)-H_2O system, PhD Thesis, Université de Bourgogne, Dijon, 2012.
[94] X. Cong, R.J. Kirkpatrick, Effects of the temperature and relative humidity on the structure of C-S-H gel, Cement and Concrete Research 25 (1995) 1237-1245. https://doi.org/10.1016/0008-8846(95)00116-T
[95] N. Baghdadi, J.F. Seignol, R.P. Martin, J.C. Renaud, F. Toutlemonde, Effect of early age thermal history on the expansion due to delayed ettringite formation: experimental study and model calibration, AGS'08, Euro Mediterranean symposium on Advances in Geomaterials (2008) 657-661.

[96] R.P. Martin, C. Bazin, J. Billo, M. Estivin, J.C. Renaud, F. Toutlemonde, Experimental evidence for understanding DEF sensitivity to early-age thermal history, RILEM-JCI International Workshop on Crack Control of Mass Concrete and Related Issues Concerning Early-Age of Concrete Structures (2012).
[97] L. Graf, Effect of relative humidity on expansion and microstructure of heat-cured mortars RD139, Portland Cement Association, Skokie, Illinois, USA, 2007.
[98] M. Al Shamaa, S. Lavaud, L. Divet, G. Nahas, J.M. Torrenti, Influence of relative humidity on delayed ettringite formation, Cement and Concrete Composites 58 (2015) 14-22. https://doi.org/10.1016/j.cemconcomp.2014.12.013
[99] R.L. Day, The effect of secondary ettringite formation on the durability of concrete, A Literature Analysis of Portland Cement Association, Skokie, Illinois, USA, 1992.

Appendix A: All results for P2 (similar to those obtained on P1).

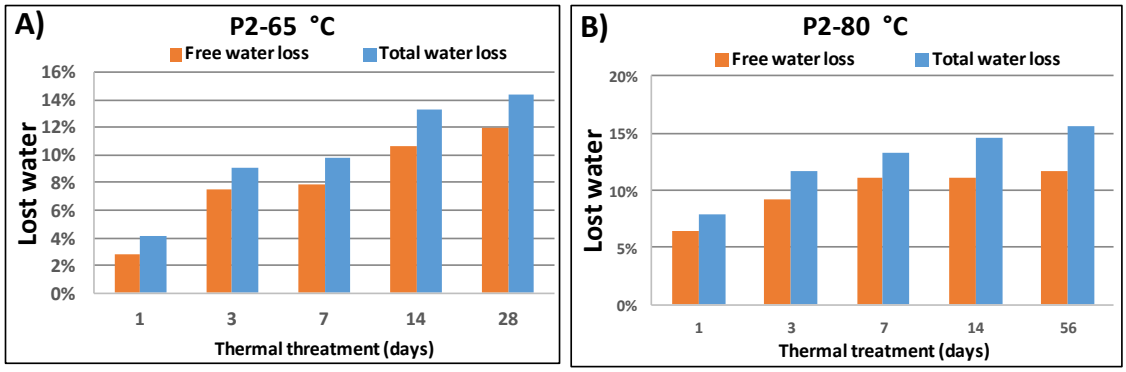

Figure A.1. Free water loss and total water loss induced by the TT for sample P2.

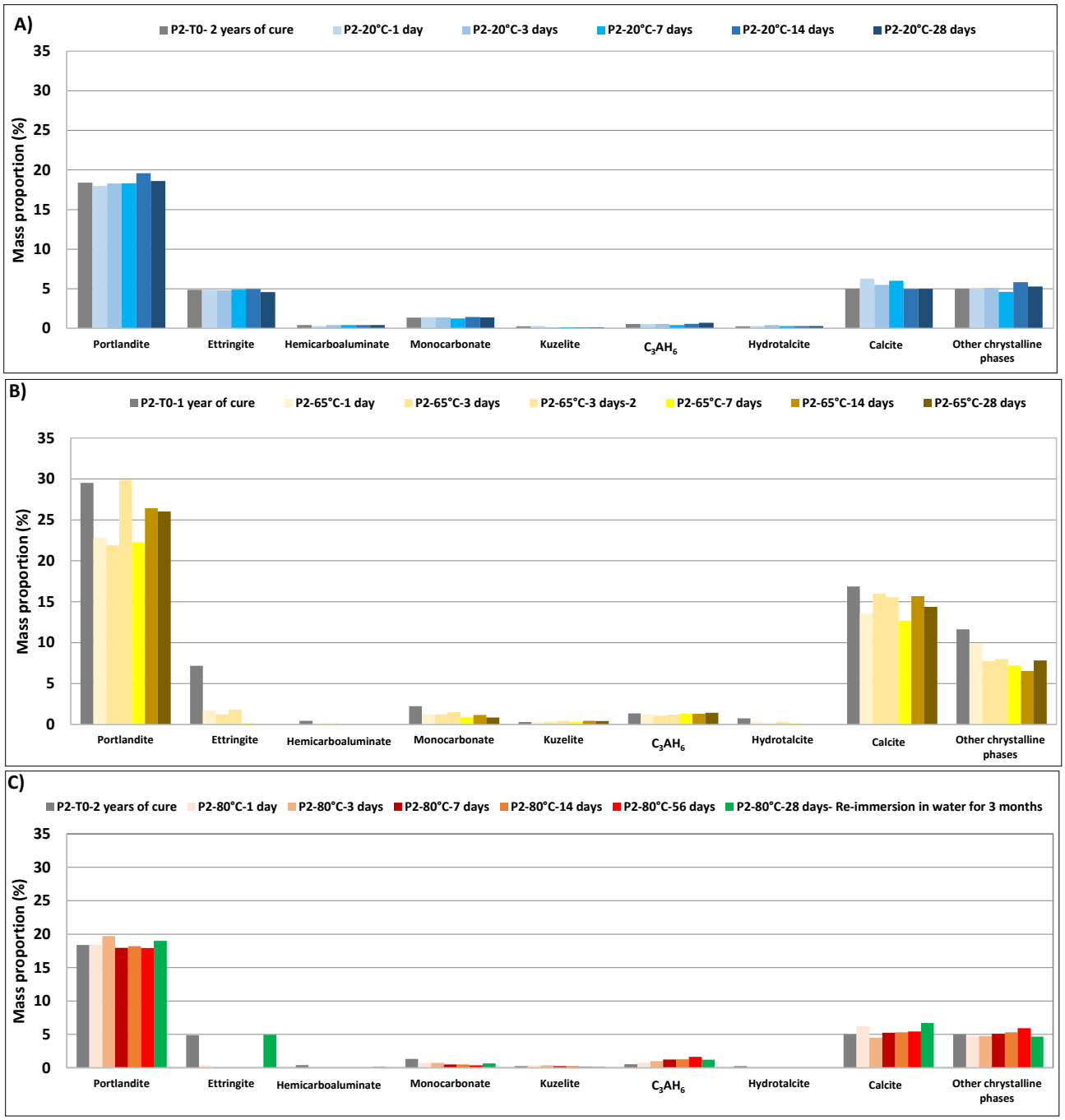

Figure A.2. Evolution of the phase assemblage as a function of the TT obtained by quantitative XRD for sample P2. The mass proportion of the phase is reported to the quantity of the initial anhydrous content. Other crystalline phases: C_3S, C_2S, C_3A, C_4AF.

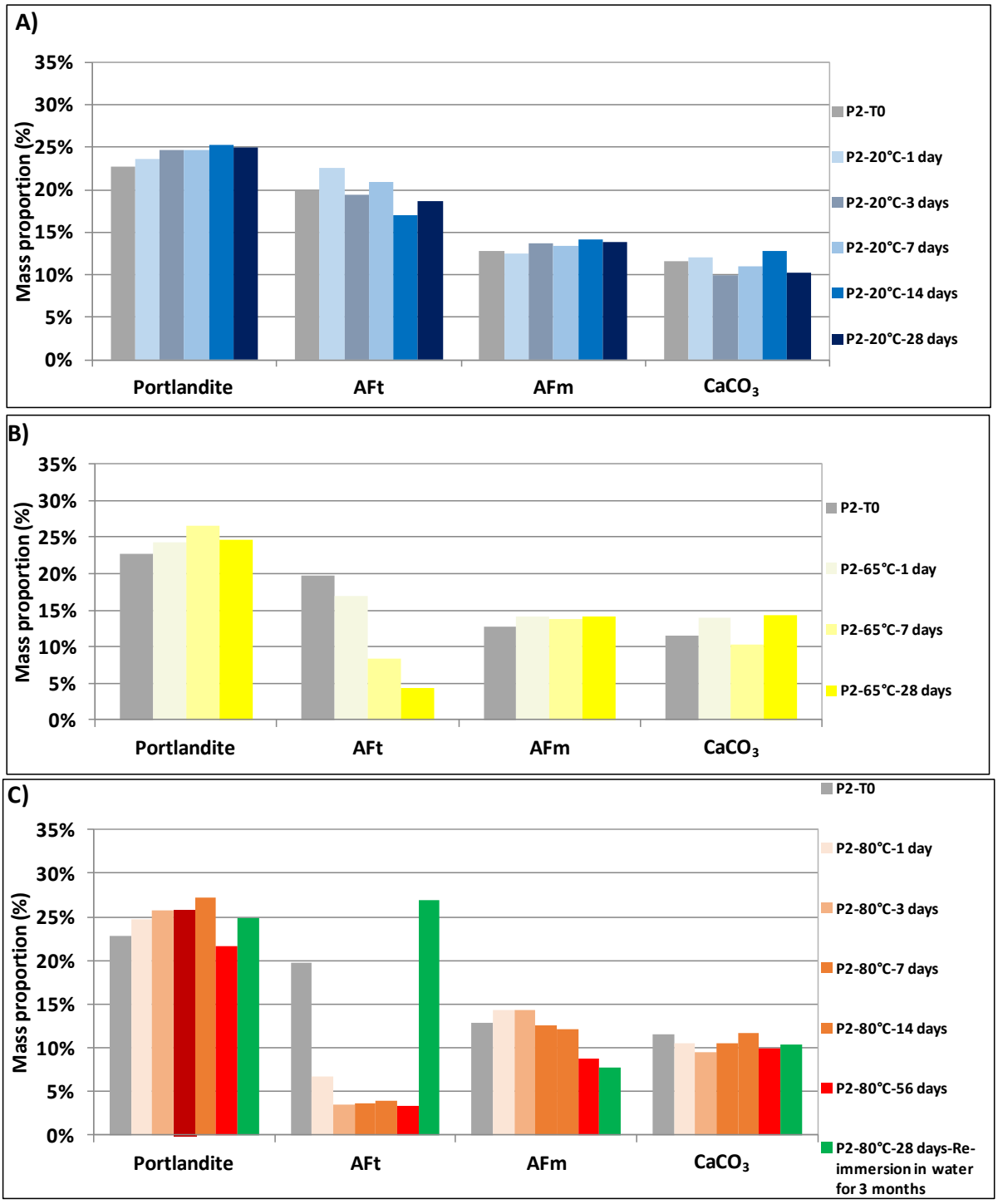

Figure A.3. Evolution of the phase assemblage as a function of the TT obtained by the combined method for sample P2. The mass proportion of the phase is reported to the quantity of the anhydrous.

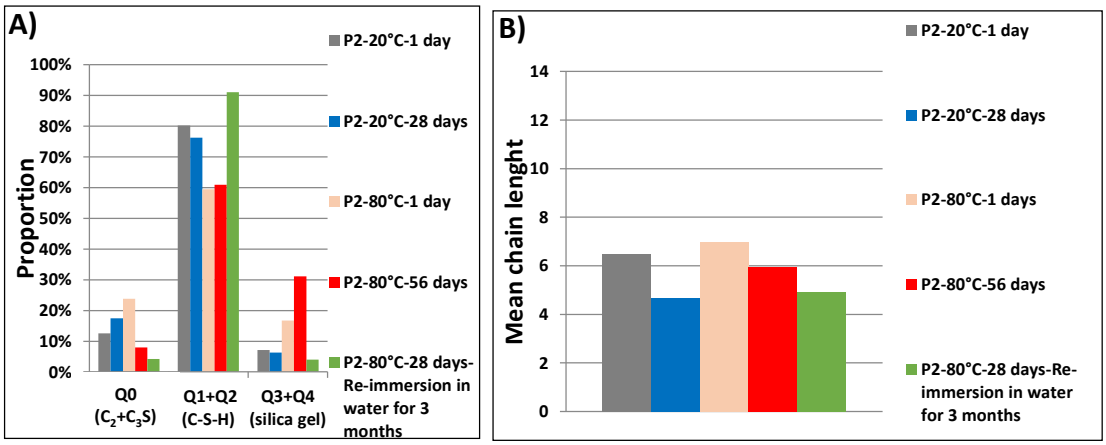

Figure A.4. Polymerization of C-(A)-S-H and silica chain length in sample P2 as a function of the applied TT obtained by ^{29}Si NMR.

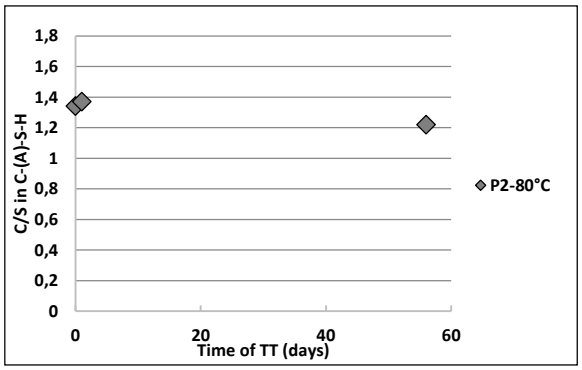

Figure A.5. Variations of the C/S ratio in the C-(A)-S-H for sample P2 during the TT.

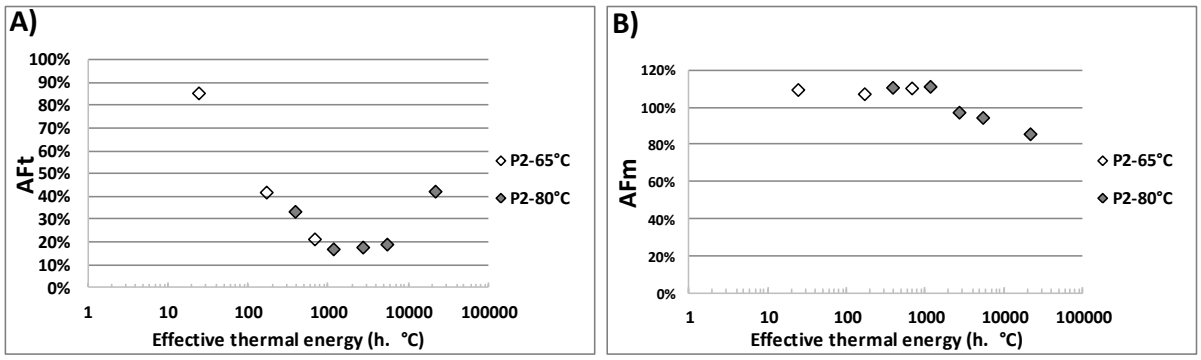

Figure A.6. Relative variations of the AFm and AFt content in sample P1 as function of the effective thermal energy.

Appendix B: Partial XRD patterns.

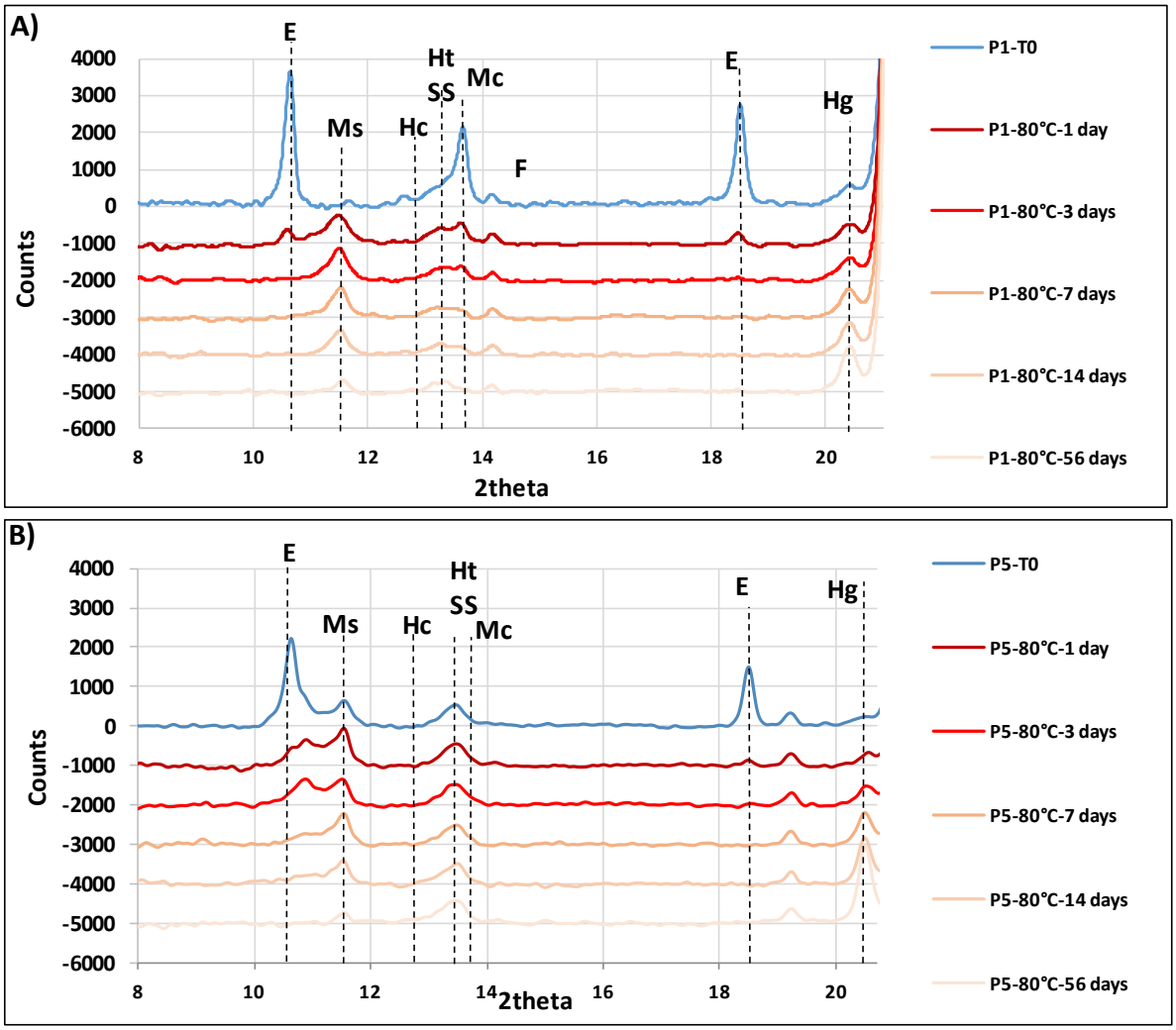

Figure B.1. Comparison of the partial XRD patterns as function of the TT of samples P1 and P5. E=Ettringite, Ms=Monosulfoaluminate, Hc=Hemicarboaluminate, Mc=Monocarboaluminate, F=C_4AF, SS= solid solution, Ht=hydrotalcite et Hg=Hydrogarnet.